MICROSTRUCTURE AND MECHANICAL PROPERTIES OF POROUS COPPER AND COPPER BRAZED WITH CU-BASED FILLER METAL

MIAN MUHAMMAD SAMI

FACULTY OF ENGINEERING
UNIVERSITY OF MALAYA
KUALA LUMPUR

2021

MICROSTRUCTURE AND MECHANICAL PROPERTIES OF POROUS COPPER AND COPPER BRAZED WITH CU-BASED FILLER METAL

MIAN MUHAMMAD SAMI

SUBMITTED IN FULFILMENT OF THE REQUIREMENTS FOR THE DEGREE OF MASTER OF ENGINEERING SCIENCE

FACULTY OF ENGINEERING
UNIVERSITY OF MALAYA
KUALA LUMPUR

2021

UNIVERSITY OF MALAYA

ORIGINAL LITERARY WORK DECLARATION

Name of Candidate: Mian Muhammad Sami [redacted]

Matric No: KGA 150044

Name of Degree: Master of Engineering Science

Title: Microstructure and Mechanical Properties of Porous Copper and Copper Brazed with Cu- Based Filler Metal

Field of Study: Advance Manufacturing Processes

I do solemnly and sincerely declare that:

(1) I am the sole author/writer of this Work;
(2) This Work is original;
(3) Any use of any work in which copyright exists was done by way of fair dealing and for permitted purposes and any excerpt or extract from, or reference to or reproduction of any copyright work has been disclosed expressly and sufficiently and the title of the Work and its authorship have been acknowledged in this Work;
(4) I do not have any actual knowledge nor do I ought reasonably to know that the making of this work constitutes an infringement of any copyright work;
(5) I hereby assign all and every rights in the copyright to this Work to the University of Malaya ("UM"), who henceforth shall be owner of the copyright in this Work and that any reproduction or use in any form or by any means whatsoever is prohibited without the written consent of UM having been first had and obtained;
(6) I am fully aware that if in the course of making this Work I have infringed any copyright whether intentionally or otherwise, I may be subject to legal action or any other action as may be determined by UM.

Candidate's Signature [redacted] Date: 08 February 2021

Subscribed and solemnly declared before,

Witness's Signature Date:

Name:

Designation:

ABSTRACT

In recent time, the heat dissipation rate of electronics increased due to the high volumetric power density they experience. In such circumstances, cooling devices with high heat transfer performance are required. Therefore, adopting porous metal can be critical in applications requiring thermal management due to its large internal surface area and high permeability for fluids. The cooling system can be composed of porous copper to enhance heat transfer making it suitable for replacement in active cooling systems, such as heat sink and heat exchanger. Effective joining of porous copper (Cu) to a copper substrate is significant when considering porous copper in the design of active cooling systems. In this research, brazing is conducted to join porous copper to a copper substrate using one piece of filler metal placed at the base side to join the base and the top side. Only one piece of filler is used to prevent the brazing material from entirely filling the cells. This method of joining two sides of metal using a single piece of filler metal with porous copper in the middle has not been studied previously. The influence of brazing parameters on the microstructural and mechanical properties of copper brazed with porous copper using amorphous filler metal (Cu-9.7Sn-5.7Ni-7P) is investigated. Brazing was done in a tube furnace equipped with a heating controller and argon gas. The brazing temperatures used in this experiment were 660 °C, 680 °C and 700 °C. The holding time was 5, 10 and 15 min. After brazing, the microstructure characterization was performed using Scanning Electron Microscope equipped with Electron Dispersive X-ray Spectroscope. To confirm the microstructure results, further analysis was conducted with X-Ray Diffractometer. It was observed that, after increasing holding time and temperature, voids or cracks were not visible in the overall bonded region. High diffusion of filler metal was also observed at porous copper surface. The diffusion between copper (Cu), nickel (Ni), tin (Sn) and phosphorus (P) created strong interactions. The EDS analysis revealed that phosphorus and nickel were

the main elements contributing to the microstructure formation. The microstructure of the brazed joints changed with increasing holding time and the diffusion of P-rich and Ni-rich phases to the upper side of the joint was observed. The element Sn completely diffused from the bonding area into the base metal due to the lower melting temperature. A further analysis was conducted to investigate the mechanical properties of porous copper and joint interface by conducting hardness and compression tests. The phases formed reduced the ductility of copper due to surface hardening effects at the brazed joint interface and porous copper. It was noticed that the rigidity of porous copper increases with increasing holding time and temperature. This is due to the diffusion of elements from the brazing filler metal into the porous copper surface. The rigidity of porous copper after brazing is vital to ensure minimal deformation of porous copper during cooling device servicing, an integral feature of prospect product development.

Keywords: brazing; porous copper; copper foam; microstructure; amorphous

ABSTRAK

Dalam tahun-tahun kebelakangan ini, kadar pelesapan haba dalam peranti elektronik telah meningkat disebabkan ketumpatan kuasa volumetrik yang sangat tinggi. Dalam keadaan sedemikian, peranti penyejukan dengan prestasi pemindahan haba yang tinggi diperlukan. Oleh itu, penggunaan logam berliang boleh menjadi kritikal dalam aplikasi pengurusan terma kerana kawasan permukaan dalaman yang besar dan kebolehtelapan yang tinggi untuk cecair. Sistem penyejukan boleh terdiri daripada tembaga berliang untuk meningkatkan pemindahan haba. Kekonduksian haba tinggi tembaga menjadikannya sesuai untuk digantikan dengan peranti pendinginan aktif, seperti penenggelaman haba dan penukar haba. Kejayaan pateri keras tembaga (Cu) berliang kepada plat Cu adalah penting sekiranya mempertimbangkan Cu berliang dalam reka bentuk alat penyejukan seperti penukar haba. Dalam kajian ini, pateri keras dilakukan untuk menghubungkan Cu berliang kepada plat Cu menggunakan sekeping logam pengisi untuk memateri bahagian bawah dan atas bagi menghalang bahan pateri keras dari mengisi keseluruhan sel. Kaedah untuk menyertai kedua-dua belah logam menggunakan sekeping logam pengisi dan Cu berliang di tengah-tengah ini adalah kaedah baharu. Pengaruh parameter proses pateri keras tembaga kepada tembaga berliang menggunakan logam pengisi amorfus (Cu-9.7Sn-5.7Ni-7P) kepada sifat mikrostruktur dan mekanikal telah disiasat. Pateri keras dilakukan menggunakan relau tiub yang dilengkapi dengan pengawal pemanasan dan gas argon. Suhu pateri keras yang digunakan dalam eksperimen ini ialah 660 °C, 680 °C dan 700 °C. Masa pateri keras adalah 5,10 dan 15 minit. Selepas pateri keras, mikrostruktur dianalisis dengan menggunakan Mikroskop Pengimbasan Elektron yang dilengkapi dengan Spektroskop X-ray Serakan Elektron. Untuk mengesahkan hasil mikrostruktur, analisis selanjutnya dilakukan dengan Pembelauan X-Ray. Selepas meningkatkan suhu dan masa pateri keras, tiada lompang atau keretakan diperhatikan, dan penyebaran logam pengisi yang

lebih tinggi telah dicatatkan di kawasan sambungan, secara keseluruhan. Penyebaran antara tembaga (Cu), nikel (Ni), timah (Sn) dan fosforus (P) menghasilkan interaksi yang kuat. Analisis EDS mendedahkan bahawa fosforus dan nikel adalah unsur utama yang menyumbang kepada pembentukan mikrostruktur. Adalah diperhatikan, struktur mikro dari kawasan sambungan berubah dengan peningkatan masa pegangan dan penyebaran fasa yang kaya dengan P dan Ni ke bahagian atas sambungan. Unsur Sn sepenuhnya tersebar dari kawasan sambungan ke dalam logam dasar kerana suhu lebur yang lebih rendah. Analisis selanjutnya dijalankan untuk menyiasat sifat mekanik tembaga berliang dan antara muka sambungan. Fasa-fasa yang terbentuk mengurangkan kemuluran tembaga dan dengan itu meningkatkan kekerasan kawasan sambungan dan tembaga berliang. Telah diperhatikan bahawa ketegaran tembaga berliang cenderung meningkat dengan peningkatan suhu dan masa pateri keras kerana penyebaran unsur dari logam pengisi pateri keras melalui tembaga berliang. Ketegaran tembaga berliang selepas pateri keras adalah penting dalam memastikan kecacatan minimum semasa servis peranti penyejukan, yang merupakan ciri penting dalam pembangunan prospek produk.

Kata kunci: pateri keras; tembaga berliang; tembaga buih; mikrostruktur; amorfus

ACKNOWLEDGEMENTS

I want to express my heartfelt gratitude to my supervisors, Dr. Tuan Zaharinie, Dr. Farazila Yusof and Prof. Tadashi Ariga. The knowledge provided by them has been of great value to me. This research was funded by University of Malaya Research Fund Assistance (BKP), grant number BK005-2015 and I am grateful for the support provided. I am also grateful for the financial support provided by the International Graduate Research Assistance Scheme (IGRAS). I would also like to take this opportunity to gratefully acknowledge the support of the AMMP Centre and Faculty of Engineering staff for making this possible. Finally, I would like to thank my mother for her prayers and endless support in all situations.

TABLE OF CONTENTS

LIST OF FIGURES

LIST OF TABLES

LIST OF SYMBOLS AND ABBREVIATIONS

Ar	:	Argon
At. %	:	Atomic Percentage
Be	:	Beryllium
B	:	Boron
C	:	Carbon
C	:	Celsius
cm	:	Centimeter
Cr	:	Chromium
Cu	:	Copper
°	:	Degree
EDM	:	Electrical Discharge Machining
EDS	:	Energy Dispersive Spectroscopy
Min	:	Minutes
mm	:	Millimeter
MPa	:	Mega Pascal
Ni	:	Nickel
O	:	Oxygen
P	:	Phosphorous
Pa	:	Pascal
PPI	:	Pores per Inch
Rpm	:	Revolution per Minute
SEM	:	Scanning Electron Microscopy
Sn	:	Tin
T	:	Temperature

Ti	:	Titanium
UTM	:	Universal Testing Machine
Wt. %	:	Weight Percentage
XRD	:	X-Ray Diffractometer

LIST OF APPENDICES

CHAPTER 1: INTRODUCTION

This Chapter introduces the background of this study to clearly explain the aim of this research. The materials used in the experiment and the procedure are briefly explained in this chapter. In addition, objectives, scopes, and limitations of this study are clarified.

1.1 Background of Study

Thermal management is a major issue for high power electronic devices facing major challenges under this trend of miniaturization and growing capacity. Generally, a cooling device with large heat transfer rate needs to be attached with an electronic device for optimum temperature level. The cooling system in electronic device is crucial for optimal performance and extended operational life span of the device. Porous metals can be critical in applications requiring thermal management due to its large internal surface area and high permeability for fluids. The thermal conductivity of the material used plays a vital role to develop equipment associated with energy efficient heat transfer process. Porous Cu is an ideal metal for use in heat sinks and heat exchangers due to high thermal conductivity of Cu and its previous use in industry for this purpose. The cooling system can be composed of porous Cu to enhance heat transfer making it suitable for replacement as active cooling devices (i.e. heat exchangers and heat sinks) (Zhang et. al., 2009; Xiao & Zhao, 2013).

Among different types of heat sinks available, those utilizing micro-channels are anticipated to have exceptional cooling performances due to higher heat transfer capacity obtained with smaller channel diameters (Ogushi et. al., 2006). Porous materials have considerable preference for three dimensional micro-channels as a heat transfer medium and several methods can contribute to heat transfer augmentations. Applications to electronics cooling of porous metal heat exchangers have been explored

by several researchers revealing promising improvements in heat transfer rate. Recently, metal foams are being analyzed as a promising alternative for compact heat exchangers and heat sinks due to advanced thermodynamic characteristics and good mechanical properties. As compared to conventional materials, the most prominent feature of porous metal is the existence of pores in the material which makes it light weight. These pores are known to have noteworthy physical and mechanical properties such as high surface area, resistance to thermal shock, and excellent noise attenuation. Some of these properties clearly indicate a potential to produce cooling devices from porous Cu (Zhao & Tassou, 2009; Ji & Xu, 2012; Mancin, et al., 2012).

1.2 Problem Statement

In conjunction with the development of cooling devices and utilization of porous material in the cooling devices design, joining of porous Cu to Cu becomes significant. Porous Cu has greater potential for many applications of which thermal properties are likely to attain breakthrough. The conventional method of cooling has been unable to meet the soaring heat dissipation requirement, all of which encourages the advent of various new cooling technologies (Zhang et. al., 2013). Researchers have worked tirelessly for decades to develop effective heat transfer equipment for use in industry. Recently, there has been substantial research to emphasize superior heat transfer capabilities of porous Cu by several researchers (Qu et al., 2012, Chiba et al., 2004). Therefore, the importance of achieving a quality metal to metal bond by brazing is ideal for heat exchangers to prevent leakage of fluids. Brazing is unique compared to other joining processes because it permanently joins base metals together with great strength. In this research, Cu-based filler metal containing phosphorus will be used to join porous Cu to Cu.

Brazing porous Cu with Cu substrate is new in the industry. Previously, joining of porous Cu has been performed using different adhesives (Joen et al., 2010). The joining of porous Cu is difficult due to its complex shape. Due to its unique characteristic (soft, porous structure and high melting point), it is difficult to determine optimum parameter for this purpose. Therefore, in this research, brazing time and temperature were manipulated to observe the effects on microstructural and mechanical properties.

1.3 Objectives

i. To investigate the changes in the microstructure of porous Cu and joint interface after brazing at different parameters.

ii. To evaluate the mechanical properties of porous Cu after brazing by performing hardness and compression test.

1.4 Scope and Limitations

The joining of two materials is important in the manufacturing of any product. If building anything that uses metal, one crucial need is to join metals together. There are many different joining processes such as brazing, welding, soldering, and bolting. However, brazing is unique compared to other joining process because it permanently joins base metals together without melting the base metals and has great strength. It is also effective for joining dissimilar metals and materials with large surface area. The main scope of this study is to join Cu substrate to porous Cu on both sides to form a sandwich structure using a single piece of filler metal placed at the base side. In this research, Cu-based amorphous filler metal will be used as brazing filler metal to join porous Cu to Cu. The filler metal will be melted, and it will diffuse into the porous Cu and top side Cu substrate for joining to occur. The study will focus on the formation of the joints to observe the microstructure and diffusion of filler metal at different brazing parameters. The mechanical properties will be investigated by hardness and

compression tests. It is expected that the porous Cu will retain its structure after brazing due to the diffusion of filler metal during brazing and then create a surface hardening effect on the porous Cu. The retained structure of porous Cu after brazing is important for the future design of cooling devices.

While conducting the experimental study, several limitations were found. Firstly, the porous Cu can only be cut using EDM wire cutting machine. This is because porous Cu is relatively soft and cannot withstand high pressure during cutting. The porous Cu can also be damaged due to high clamping force required in other methods. The brazing temperature selected in this study was higher than the liquidus temperature of the filler metal. As the filler can be placed on one side of Cu substrate only to avoid filling the pores of porous Cu, the brazing temperature had to be on higher side to achieve diffusion towards top side Cu substrate. The brazing process employed relatively lower temperatures and shorter holding times to make the process economical and promote lean manufacturing initiative. Furthermore, the brazing process takes about 5 hours to complete until the cooling stage. Due to this, only one sample parameter can be set per day. Three samples of each parameter were required to carry out the experiments. Therefore, EDS and micro hardness test was carried out for all parameters. Based on the analysis from EDS and micro hardness test, remaining experiments were carried out for selected parameters. Since brazing process requires protective atmosphere, argon gas is used. However, as Cu can oxidise quickly, longer processing time caused large amount of gas to be used per sample (American Welding Society, 1991).

1.5 Organization of Report

This report is organized according to chapters. The descriptions of the chapters and its contents are briefly explained below.

- Chapter 1

Chapter one introduces the background of this study to clearly explain the aim of this research. The materials used in the experiment and the procedure are briefly explained in this chapter. In addition, objectives, scopes and limitations of this study are clarified.

- Chapter 2

This chapter focuses on the literature review based on previous research related to this study. Hence, this chapter is the basis for the study to understand the theory and gives guidance to proceed with experiment.

- Chapter 3

This chapter describes all the experimental procedure involved in this research and previous literature related to the experiment. It mainly describes the type of materials, measurements, machines and set up parameters required for the experiment.

- Chapter 4

This chapter represents the results and discussion obtained from the experiment. All the findings and data gathered from the experiment are discussed thoroughly in this chapter. The results are presented in the form of images, tables and graphs.

- Chapter 5

This chapter concludes the overall results and discussion made earlier. This chapter also provides recommendations for future studies.

CHAPTER 2: LITERATURE REVIEW

This chapter focuses on the literature review based on previous research related to this study. Hence, this chapter is the basis for the study to understand the theory and gives guidance to proceed with experiment.

2.1 Introduction of Materials used in this Research

Pure Cu is well known metal for its mechanical properties and has been used in industry extensively. Production of wires, integrated circuits, heat sinks, and heat exchangers are examples of Cu applications in many branches of industry. Due to unique properties such as heat conductivity and high electrical conductivity makes Cu widely applied in engineering (Liu et. al., 2008). Moreover, Cu is soft, malleable and ductile material. Therefore, it can be shaped into thin sheets, drawn into wires and made into pipes. In the second half of last century, detail studies regarding the mechanical properties and microstructure in relation to Cu have been performed.

2.1.1 Porous Copper

As for porous Cu, it is often called lotus-type porous or gasar materials. It is a type of Cu that is made up of straight elongated pores, which can be manufactured by the precipitation of supersaturated gas dissolved in the molten metal during solidification (Nakajima, 2007). Porous metal is also known as “metal foam” or “cellular metal” in some literatures. It can be classified as (i) an open-cell or closed-cell structure; or as (ii) a stochastic or ordered/periodic configuration. Open-cell porous metal comprises of cells that are all interconnected permitting a fluid to pass through. However, in closed-cell porous metal, an individual enclosure is created by the cells within the material. Stochastic porous metal structures are clearly very different from the periodic orientation of pores. As compared to conventional metals, the most prominent characteristic of porous metal is the presence of many voids within the material. These

porous metals have many interesting combinations of physical and mechanical properties (Tuchinskiy, 2005) including:

i. Light weight (comprised of about 90% of air).

ii. High to very high specific surface area (from 500 - 10,000 m2/m3).

iii. High thermal conductivity combined with high gas permeability.

iv. Resistance to high temperature, wear, thermal shock, and humidity.

v. Good energy absorption capacity.

vi. High strength and suitable for high-pressure conditions.

vii. Control over material morphology (pore size and distribution).

viii. Excellent fluid mixing due to tortuous flow path.

ix. Excellent noise attenuation.

A few of these listed properties certainly imply a potential to develop cooling devices as investigated by several researchers (Zhao & Tassou, 2009; Ji & Xu, 2012; Mancin, et al., 2012) and these devices often constructed using Cu, aluminium or steel (T'Joen et al, 2010). However, the cooling devices are normally operated in both natural and forced convection. Porous metal application into fin-and-tube designs has proved to be more challenging because of the large pressure drop observed on the air side. Therefore, alternative designs are required, in which the material properties utilize their potential. Hence, the joining condition also needs to be considered for the cooling device made up of porous metal.

Vesenjak et al., (2012) stated that due to low density of the material, and high capacity of energy absorption makes porous Cu valuable in novel designs of lightweight structures. The planned structure of lotus-type porous metal can contribute to the mechanical properties that can be categorized by length of pores, direction of pores, and the ratio of pore size to distance between pores (porosity). However, these parameters define the porous metal structure only to a specific extent. This is because the volume slightly varies in production. The pores have irregular cylindrical shapes in actuality, and their size and lengths are not identical. Figure 2.1 shows porous Cu with different types of porosity.

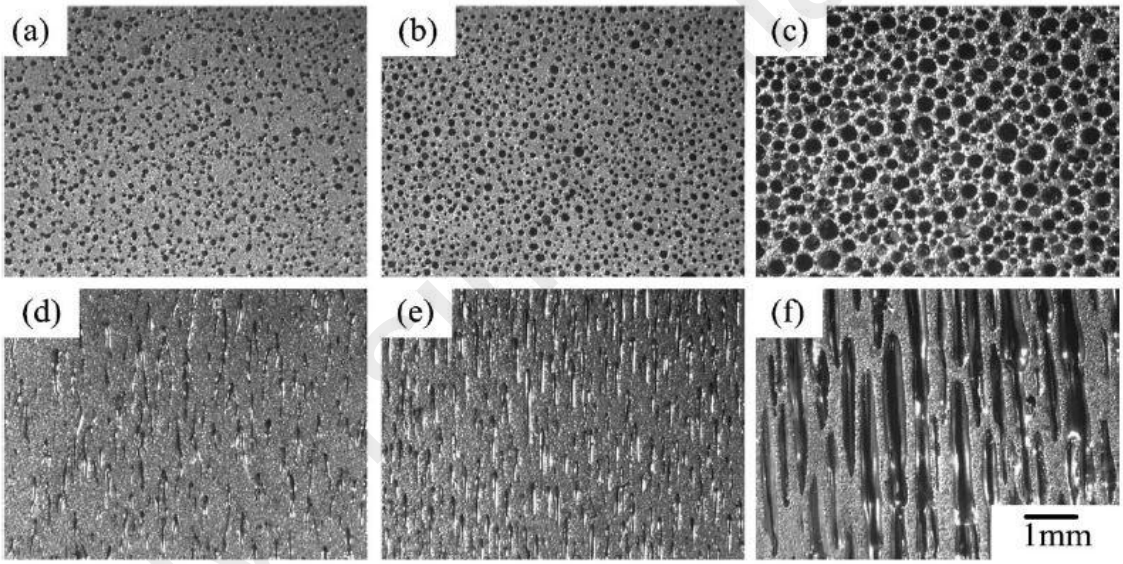

Figure 2.1: Micrographs of porous Cu with (a), (d) 22.0% porosity, (b), (e) 31.4% porosity and (c), (f) 53.3% porosity. (a), (b) and (c) are sections perpendicular to the pore axis, while (d), (e) and (f) are those parallel to the pore axis (Hyun et al., 2004)

2.1.2 Copper-based Brazing Filler Metal

In this research, Cu-based filler metal known as MBF2005 was used for brazing porous Cu to Cu substrate. The amorphous filler has several combinations of other materials such as nickel, tin and phosphorus. A similar filler metal was used by Zhang et al. in their research to join graphite and Cu. However, in this case chromium was used instead of tin (Zhang et al., 2014). As Ni-based filler alloys have strong corrosion

resistance and creep strength, a novel Ni-Cr-P-Cu filler alloy was developed to join graphite and Cu. In order to address the joining problem with Cu, the mutual solubility of Cu and Ni due to the same crystal structure and similar radii is valuable. The melting point in the filler metal can be reduced efficiently by the P element according to the Ni-P binary phase diagram (Schmetterer et al., 2009). In addition, the spreading ability and wettability of the filler metal can be improved by P (Zorc & Kosec, 2000). By adding Cu in the filler metal, the electrical conductivity of the bonded region can be improved to a certain level because of low electrical resistivity.

Pure metals usually have defined melting points, but the transformation from solid to liquid state for most metal alloys take place within a certain zone. The working temperature relies on the chemical composition of the brazing filler metal. The advantage of this filler metal (MBF2005) is low liquidus temperature which allows brazing to be performed at lower temperature.

2.2 Production of Porous Copper

Generally, the pores have unique functions such as channels of supply, light weight structure and fluid permeability. Due to the wide surface area resulting from high porosity, these penetrated pores can be used as electrode materials for filtering and utilization. Moreover, porous materials are in high demand for several applications of lightweight structural and functional materials. Nakajima (2007) had studied about the expansion of manufacturing method, properties of porous metals and their applications. He explained that unidirectional solidification in the pressurized gas atmosphere, such as oxygen, nitrogen, and hydrogen produced porous Cu. As the molten metal dissolving the gas is solidified, the pores evolve from insoluble gas. The ambient gas pressure and solidification velocity were able to control the pore size and porosity, whereas the pore direction is controlled by solidification direction. A special kind of micro-channel heat

sink can be produced using porous Cu as it possesses high thermal conductivity and large surface area.

2.3 Brazing Process

Brazing is a metal joining process in which two metals are joined together by melting a filler metal into the joint. Generally, there are many techniques of brazing that are performed in brazing furnace. It is a process by which the parts or assemblies being joined are heated to the melting point of the filler metal being used, but below the melting point of the base metals to be joined. The liquid metal flows into the desired joint region by capillary action after heating to the melting temperature of the filler metal and solidifies upon cooling to create a leak-proof bond. Typically, the melting temperature for filler metal is above 450 °C. Brazing can be distinguished from soldering by temperature. Soldering temperatures and joining strength are lower than brazing (Kalpakjian, 2006). A successful brazed joint often results in a metallurgical bond that is generally as strong as the base metals being joined. Furnace brazing is often selected due to its effectiveness in preventing oxidation. The equipment allows the introduction of an inert gas such as argon which passes through the tube. Argon gas creates a protective atmosphere to prevent oxidation (American Welding Society, 1991).

2.3.1 Furnace Brazing (Brazing Environment)

Furnace brazing is a semi-automatic process applied extensively in industrial operations because of its adaptability to mass production. The advantage of using brazing over other metal-joining techniques is its ability to braze complex and multi-part assemblies cost effectively. Examples of difficult assemblies include odd shapes such as porous structure, thick and thin section, and cast alloys that can be made into integral components by a single trip treatment in a brazing furnace. Among new joining

techniques, brazing has received widespread attention due to its joint strength, low cost-effectiveness, good repetitiveness, as well as flexibility of joint size and shape.

Vacuum furnaces can be equipped to allow the introduction of an inert gas such as argon to increase the pressure to create a so-called partial vacuum atmosphere. The advantages of using an industrial gas-based brazing atmosphere are consistency, safety and the ability to precisely control the composition of the furnace atmosphere. All of the brazing atmosphere types control oxide formation within the heating chamber, and even act to break down existing oxides. Many types of ferrous and non-ferrous base metals may be brazed with good results in a controlled atmosphere furnace, the most common being cast iron, steel, copper, and aluminum. Argon is useful in minimizing or preventing the volatilization of base metals or filler metals.

In this investigation, an open type of porous Cu was joined to a Cu substrate using brazing method. One piece of amorphous filler metal was placed at the base to join Cu substrate on both sides with porous Cu, creating a closed-cell sandwich structure. The emphasis of this research is to study the effects of brazing parameters (i.e. temperature and time) on brazed joint interfaces and porous Cu for application as a heat exchanger or heat sink.

2.3.2 Heating Cycle

Heating cycle can be varied according to the purpose of the experiment. For example, there are seven steps of heating cycle to braze 304 stainless steel plate-fin structures with BNi2 filler metal in a research conducted by (Jiang et al., 2010). The first step begins by pumping vacuum of the furnace to 0.001 Pa. The stacked plate-fin system is then heated within 50 minutes to 850 °C (step 2). To minimize the temperature gradient of the entire assemblies, the temperature is maintained for 30 minutes (step 3). In step four, heating is then resumed to the brazing temperature of

1050 °C within 30 minutes, leading to the best capillary flow of nickel-based filler metal. Step 5 is the holding stage, which helps the carbide of the austenitic stainless steel to attain desirable solid solution treatment. The cooling stage composes of two steps. The first is vacuum self-cooling, where the temperature falls from 1050 to 620 ° C, which takes about 40 minutes (step 6). After lowering the temperature to 620 °C, rapid cooling is carried out by filling the furnace with dry nitrogen and running the wind cooling system that lasts about 50 min (step 7). Figure 2.2 below shows the graph representing seven stages of heating cycle.

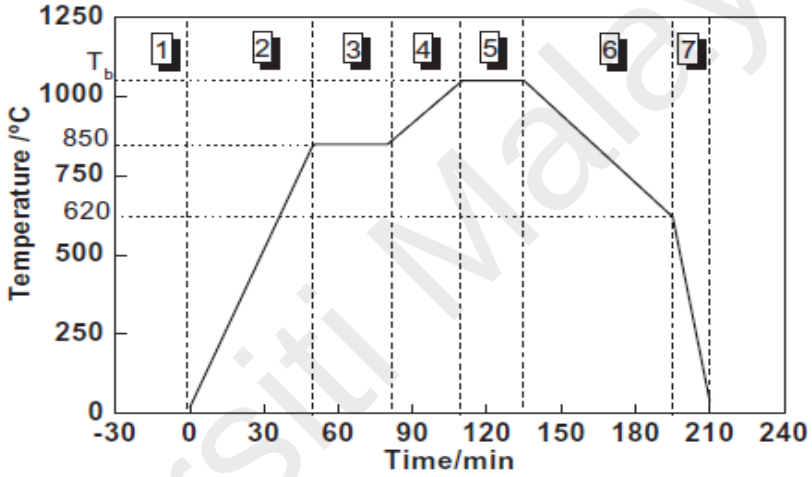

Figure 2.2: Seven stages of brazing heating cycle (Jiang et al., 2010)

Moreover, research conducted by Miab & Hadian (2014) show quite similar technique for brazing. Cubic boron nitride (cBN)/steel (CK45) joints are brazed with an active brazing alloy. The brazing process was carried out using a tube furnace under high purity argon atmosphere at a constant brazing temperature of 920 ºC. The brazing time varied between 5 and 15min. The filler alloy was sandwiched between the cBN and steel using a graphite jig. The assembly was forced into the hot zone of the furnace by using a sealed push rod system. At the end of the brazing cycle, the assembly was removed from the hot zone and cooled to room temperature under protective atmosphere. Zhang et al., (2013) explained about the brazing process cycle in their study on heat transfer performance which involves vacuum brazing. Firstly, the furnace

needs to be vacuumed (vacuum degree is 10-3Pa). Then heating process took place and the assembly was heated to a temperature of 800˚C. When the temperature reached the required temperature, it had a holding time of 10 min before cooling. The cooling process requires the sample to be kept in the vacuum furnace under protective atmosphere. Hence, basically in brazing process, the most essential steps are heating, holding and cooling.

2.3.3 Effect of Brazing Temperature and Holding Time

Technically, brazing temperature is an important parameter in determining the braze joint. Zaharinie and Co-authors (2014) vacuum brazed sapphire with Inconel 600 using Cu/Ni porous composite interlayer with a commercially available Cusil ABA (63Ag-1.75Ti-35.25Cu) filler foil as braze alloy. To decrease the residual stress occurring during the cooling stage, a porous Cu/Ni interlayer was used. A high vacuum furnace was used for brazing at 1×10^{-4} Pa vacuum pressure. The heating was performed at 830, 865 and 900 °C with a holding time of 15 and 30 min. The rate of heating and cooling were set at 5 ºC/min and 3 °C/min, respectively. At a low brazing temperature, due to high residual stress occurred during brazing at 830 ºC, the brazing failed. However, successful joining was obtained at a high temperature of 900 °C for both holding time.

The effect of brazing temperature on properties of joint also supported by study to join graphite and Cu brazed using a novel Ni–Cr–P–Cu filler alloy (Zhang et al., 2014). The brazing process was carried out in a vacuum for 10 min at various temperatures (900-980 ºC). The assembly was heated to 350 ºC at the beginning and held for 30 min to volatilize the binder. The temperature was then raised to 890 ºC and held for 20min, and later increased to brazing temperature, isothermally soaked for 10 min. Finally, the brazing samples were cooled down to 200 ºC. It can be observed that the number and size of Cu-based solid solution increase whereas the thickness of the brazing layer

reduces on elevating the brazing temperature. Therefore, faster reaction speed between elements was observed due to higher brazing temperature.

The influence of brazing temperature and time was investigated using commercially pure titanium sheet brazed with CBS34 (Ag-20Cu-22Zn-24Cd) braze filler foil to evaluate brazed joint strength and microstructure (Ganjeh et al., 2012). In this study, the brazing temperatures and holding times used were 800-870 °C and 10-20 min, respectively. According to the analysis, both the brazing temperature and the holding time are important factors for controlling the microstructure and thus the mechanical properties of the brazed joints. According to the data, sound joints were attained without any cracks or voids along joints for samples brazed at 850 °C and 870 °C. Although brazing filler metal can melt at temperature of 800 °C, evaporation of zinc and cadmium in braze alloy established voids in brazed joint due to low melting points. Therefore, at higher temperature they evaporated, and the porosity remained in the joint. As a result of the diffusion of Cu atoms from the braze alloy into the Ti substrate, the amount of Ti_2Cu decreases with increasing brazing temperature and/or time. The shear strength of joints increased with a rise in holding time. Brazing at 870 °C, 20 min established uniform distribution hardness compared to other brazing temperatures. The optimum brazing parameter was obtained at 870 ºC, 20 min as highest shear strength was obtained.

Miab & Hadian (2014) had conducted research to study the effect of brazing time on microstructure and mechanical properties. In order to join stainless steel with Cusil-ABA, they used cubic boron nitride. The brazing process was conducted in a high purity argon atmosphere using a tube furnace at a constant temperature of 920 ºC. The brazing time ranged between 5 to 15 min. During their research, they found that by increasing the brazing time will cause the changing of microstructure brazed layer. By increasing

the brazing time, the reaction layer becomes thicker and more continuous resulting in higher joint strength. With the increasing of brazing time, the microstructure of braze layer changed significantly. The dendritic shape of the dark phase has been migrated and concentrated across the interfaces. This phenomenon can be explained by the reaction of Ti with cBN. In fact, reacting with cBN and making more wettable products is the role of Ti as an active element. In the interfacial reactions during the brazing process, the Ti element should be consumed. Longer dwelling time provides Ti with more opportunities to spread to the cBN/Cusil-ABA interface and to produce a Ti-rich phase along the interphase. Hence, as a result, increasing brazing time causes the dark phase to move and concentrate above the braze layer. On the other hand, it is appropriate to declare the change in the distribution pattern of Ti as the effect of the brazing time on the reaction layer. Therefore, they concluded that thicker and more continuous reaction layer was achieved due to longer brazing time.

Reliable alumina/Cu joints were obtained at 580–660 °C for 5 min by brazing pre-metallized alumina and Cu using SAC filler (Fu et al., 2015). It was shown that the microstructure varied clearly with the brazing temperature. The Cu–Sn intermetallic layers thickened rapidly as brazing temperature increased. It was notice that the Ti_6Sn_5 phase did not change substantially at temperature below 620 °C, however, when brazing was performed at 660 °C it disappeared. When brazing temperature was higher than 620 °C, substantial amount of Kirkendall voids and microcracks formed in Cu_3Sn layer. At brazing temperature of 620 °C, the highest average shear strength of 32 MPa was obtained. As the brazing temperature rose further to 640 ° C and 660 ° C, kirkendall voids formation caused the joints to fracture along the Cu/Cu_3Sn interface and the shear strength decreased sharply. The shear strength of the alumina/Cu joints was correlated with the microstructure of the interface that was heavily dependent on the brazing temperature.

Esmati et al., (2014) studied the microstructure and mechanical properties of diffusion brazing joint of Cu Beryllium alloy. A spreadability test was carried out at two temperatures for different metals of Ag content. For each filler metal used, by increasing the temperature, the spreadability increased. The microstructure of the brazed joint changes gradually with increasing time and temperature. Figures 2.3 show the effect of temperature on microstructure of the specimens, respectively.

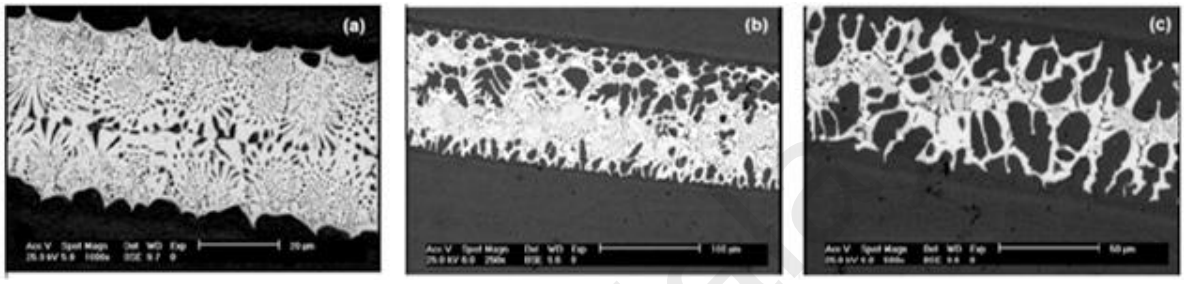

Figure 2.3: SEM BEIs of Cu Beryllium brazed for 900 s at (a) 600 ºC, (b) 700 ºC and (c) 750 ºC (Esmati et al., 2014)

The thickness of reaction layer between the brazed bond and substrate increases and the eutectic phases disappear by increasing the brazing time and temperature. The growth of interfacial reaction layer leads to loss of elements in the braze alloy. Therefore, the microstructure of the reaction layer changes with increasing brazing time and temperature. As most of Zn reacts with Cu, therefore the Zn content in the braze seam is low. By increasing time and temperature, the micro hardness values show that the hardness at center of bond zone decreases due to dissolution and interdiffusion of main elements to base metal. The effect of time and temperature on the tensile strength of brazed joint was also investigated. The tensile strength increases with the increase in bonding time up to 1200 s. For the specimen brazed at 750 ºC for 1200 s the maximum tensile strength is 173 Mpa.

Hissyam and Co-authors (2017) investigated the effects of Cu-based filler composition and brazing temperature on the spreading and wetting behaviour. MBF

2002 (Cu, 9.9wt.%Ni, 4.0wt.%Sn, 7.8wt.%P), MBF 2005 (Cu, 5.7wt.%Ni, 9.7wt.%Sn, 7.0wt.%P), and VZ 2250 (Cu, 7.0wt.%Ni, 9.3wt.%Sn, 6.3wt.%P) were used as brazing filler materials. Pure Cu block and a rectangular plate were employed as the base metal. Brazing was performed at 750 ºC and 800 ºC with holding time of 30 min. The results show that the spreading area increased with increasing brazing temperature. Furthermore, the wetting angle is higher with increasing brazing temperature.

EDS allows the elemental composition of the specimen to be measured. There are several methods when applying EDS in the experiment depending on what kind of outcome is required. Hasap, et al., (2014) uses EDS elemental mapping to investigate the microstructure of the braze joint. Figure 2.4 demonstrate the example of elemental mapping result that was obtained.

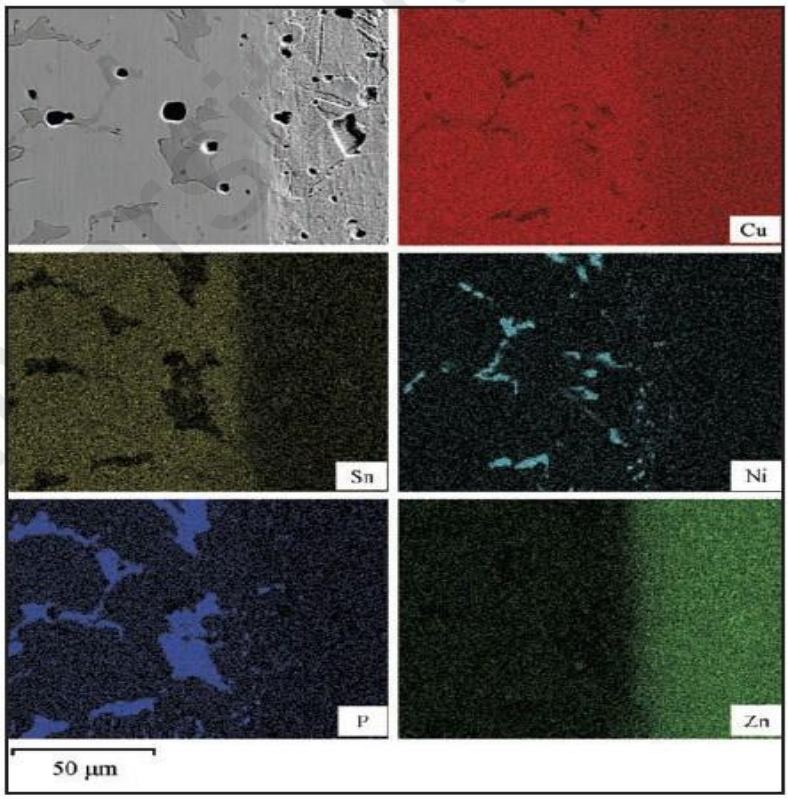

Figure 2.4: Micrograph and EDS elemental mapping of Cu brazed joint (Hasap et al., 2014)

Soltani, and his team (2014) used scanning electron microscopy equipped with EDS elemental mapping to characterize the bonds. The reaction layers were formed on the shared surface of the base metals and interlayer. The magnitude of Ag-rich phase decreased with increasing the brazing temperature and time. The analytical result from the EDS analysis usually comes out in the form of weight or atomic percentage. In extension of Hasap et al., (2014) research on microstructure and strength of Cu brazing joints, the EDS analysis is shown in Figure 2.5. From the data, relationship of the weight percentage and the temperature can be investigated by referring to the phase diagram.

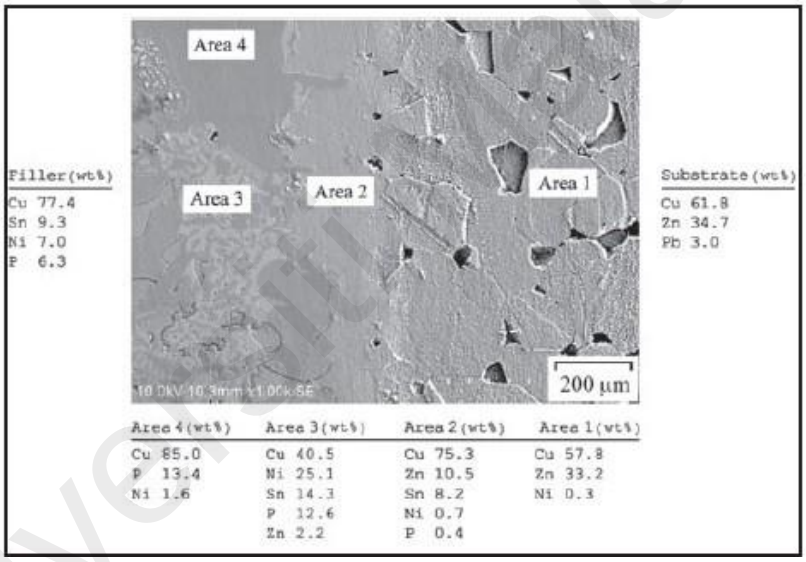

Figure 2.5: Micrograph and EDS analysis of Cu brazed joint (Hasap et al., 2014)

Jattakul & Kanlayasiri (2018) investigated the effects of brazing parameters on microstructure of Cu sheets using Cu-Ni-Sn-P amorphous filler metal. Argon gas was used to protect the sample from oxidation and the heating rate was set at 10 ºC /min. The varying brazing temperatures employed were 600 ºC, 640 ºC, 660 ºC, and 680 ºC with holding time of 5 min. After the brazing process, the microstructure and the elemental composition was examined using SEM equipped with EDS. Figure 2.6 (a-f)

shows the microstructure morphology of Cu/Cu-Ni-Sn-P/Cu joints at both low and high magnification when brazed at varying temperatures of 640 °C, 660 °C, and 680 °C.

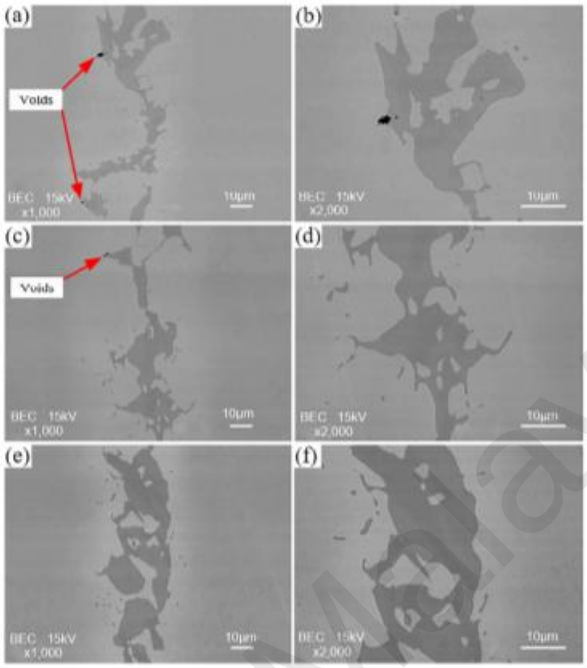

Figure 2.6: Micrograph of cross-section of Cu/Cu-Ni-Sn-P/Cu brazed joint using 5 minutes holding time at varying brazing temperatures of: (a-b) 640 °C, (c-d) 660 °C and (e-f) 680 °C (Jattakul & Kanlayasiri, 2018)

The examination revealed that there were micro-voids found between the filler metal and Cu substrate. This led to doubts about the efficiency of the joint shown in Figure 2.6 (a) and Figure 2.6 (b). The reason for this shortcoming is that filler was unable to completely react with Cu at relatively low brazing temperature of 640 ºC. Upon increasing the brazing temperature to 660 ºC (Figure 2.6(c) and Figure 2.6 (d)), the voids were minimized. Finally, at brazing temperature of 680 ºC, no cracks at all can be observed as indicated in Figure 2.6 (e) and Figure 2.6 (f). Therefore, solid joints without micro-pores or any defects at the brazed joint interface were obtained when the brazing temperature increased to 680 ºC.

Zhang et al., (2016) studied the microstructure and mechanical properties of pure Cu brazed with amorphous Cu-68.5Ni-15.7Sn-9.3P-6.5 (wt.%) Filler Metal. This study

investigated the influence of brazing parameters (temperature and time) on the interfacial microstructure and strength of brazed joints. The brazing temperature was selected in the range of 660-720 ºC and the holding time was varied from 5-30 min. The microstructure and phase composition of joints were examined using SEM. Figure 2.7 shows the interfacial microstructure of brazed joints at different temperatures for 10 min. For the joint brazed at 660 ºC shown in Figure 2.7 (a), the thickness of the residual filler metal was found to be identical to that of initial filler. This indicates the interaction between filler metal and Cu substrate is minimal due to lower brazing temperature. The joint brazed at 680 ºC formed a large amount of continuous grey phase between the Cu substrate (Figure 2.7 (b)). It was observed that Cu-P phase evidently decreases when the brazing temperature rises to 690 ºC. By increasing the brazing temperature, the dark residual filler layer becomes thinner (Figure 2.7 (c)). It was concluded that the morphology of the joints is greatly affected by the brazing temperature and time.

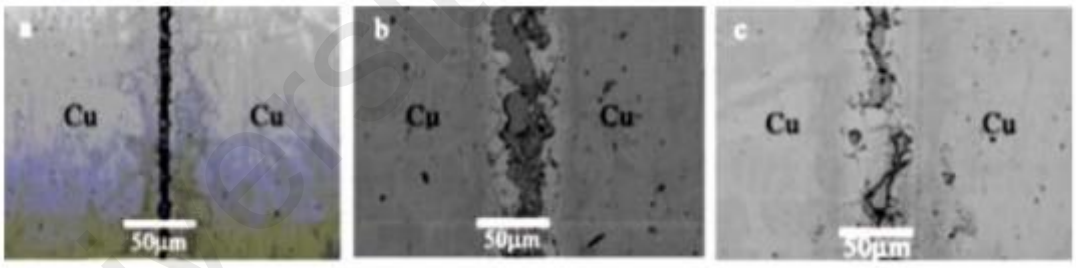

Figure 2.7: Interfacial microstructure of pure Cu brazed joints at different temperatures for 10 min (a) 660 ºC, (b) 680 ºC, (c) 690 ºC (Zhang et al., (2016)

2.4 Compression Test

The standard result of a compression test for metal foams is shown in Figure 2.8. This curve can be distinguished by three different phases. In the first region, deformation occurs elastically and presents an almost linear development of stress with strain. This elastic deformation is mainly due to flexural cell unions for low density,

open cell foams. The contribution of cellular or compression couplings becomes increasingly important as the density increases.

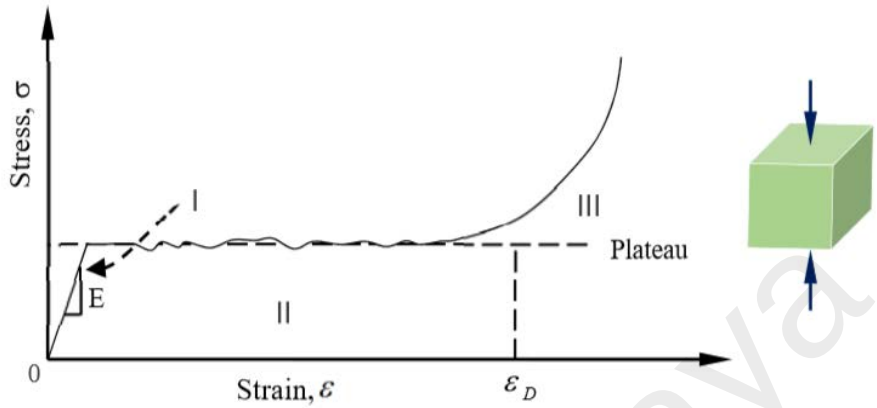

Figure 2.8: Typical compression stress-strain curve for metal foams (Ashby et al., 2000)

A practically constant stress level is shown in the second phase. The collapse of the cells corresponds to this region. The mechanism of collapse depends on the foam base material and can be a plastic collapse. When the stress surpasses a certain value, the cell collapse occurs in a plane perpendicular to the loading direction. As the deformation increases, the collapsed region will be propagated through the material. In elastoplastic foams, plastic collapse leads to an almost horizontal development in the stress-strain curve. This is a central component of cellular materials utilized in the case of energy absorption. The energy absorbed by the sample precisely correlates to the area under the stress-strain curve. The last phase of the curve is associated with material densification. The cell walls are close and come into contact as the deformation increases, leading to a rapid increase in the stress-strain curve (Ashby et al., 2000; Nakajima, 2007).

2.5 Application of Porous Copper in Heat Management Devices

Recently, porous metals are being studied as a promising alternative for heat sinks due to high surface area, density, and superior thermodynamic characteristics. Zhang et al., (2013) investigated experimentally on heat transfer performance of lotus-type

porous Cu heat sink. Zhang and his team fabricated a special kind of micro-channel heat sink using porous metal with long cylindrical pores. During sample fabrication, the lotus-type porous Cu was combined with a smooth plate of pure Cu by using two methods: (1) Diffusion welding and (2) Brazing in vacuum to form the lotus-type porous Cu heat sink testing section. In comparison to brazing, diffusion welding has a slight deformation due to applied force leading to slightly compressed pores. Therefore, brazing method was used to fabricate all heat sinks because it has higher productivity and lower cost. They reported that heat transfer performance can be directly affected by pore diameter and penetrative porosity. The penetrative porosity must be increased to realize the practical application of porous Cu heat sink. The results from the experiment show that lotus-type porous Cu heat sink has excellent heat transfer performance compared to conventional type.

Qu et al., (2012) studied the natural convection at various pore densities (10-40 PPI) and porosities (0.90-0.95) in porous Cu and observed that with decreasing pore density and porosity, the heat transfer rate increases. In addition, owing to the greater surface area, heat transfer performance is improved with increasing height. Chiba et al., (2014) studied both experimentally and analytically heat transfer capacity of lotus-type porous Cu heat sink. They investigated a fin model for predicting heat transfer capacity of three types of heat sink: with conventional groove fins, with micro-channels and with lotus-type porous Cu fins. The lotus-type porous Cu fins have pores with a diameter of 0.3mm and a porosity of 0.39. A heat transfer capacity 4 times greater than the standard groove fins and 1.3 times greater than the micro-channel heat sink under the same pumping power was observed for the lotus-type porous Cu fins. Chuan et al., (2015) proposed a new design idea using porous fins in microchannel heat sink. To reduce the pressure drop across the heat sink, the design was proposed. The simulation showed that the presence of porous fins contributes to the coolant's non-zero velocity at the interface

between the channel and porous fin, which lets the coolant act on the channel wall like a "slip". The "slip" has a drag-reducing effect which is the main reason for the reduction in pressure drop in the porous fin heat sink. The pressure drop of the new design was reduced by 43% compared to the conventional fin design. The heat transfer and pressure drop performance of metal foam heat exchangers was compared by Dai et al., (2012) to another state-of-the-art heat exchanger. Two heat exchangers were subjected to the same performance requirements in the study and the resulting volumes, masses and costs were compared. The efficiency of the metal foam heat exchanger was identical to the louvered-fin heat exchanger with a smaller and lighter design. However, the cost of the metal foam heat exchanger was much higher owing to the metal foam cost.

Another study carried out by Du et al., (2014) investigated heat dissipation performance of porous Cu with long cylindrical pores. Due to a small pressure drop of water passing through the pores, the porous metal with elongated cylindrical pores, also known as Gasars, is preferable for heat sinks. Gasars are relatively new class of porous materials produced by a solid-gas eutectic solidification process. The study showed that by forced air convection, porous Cu dissipated heat more rapidly than by normal convection. Also, it was found that both porosity and pore size play a critical role in the performance of porous Cu. The investigation concluded that porous Cu with higher porosity and pore size possesses higher heat dissipation rate. Porous material can be brazed to a thermally conducting plate or can be directly brazed to the hot surface, to use in heat transfer applications.

Investigation on convection heat transfer from aluminium and Cu foams in a vertical channel has been conducted by Pradeep et al., (2013). The effect of thickness and thermal conductivity of high porosity foams on heat transfer and pressure drop were studied. The experimental results show that increase in the foam thickness leads to a

substantial increase in heat transfer. As compared to the empty channel, metal foams enhance heat transfer by 2.6-3.8 times for the same inlet velocity. Then, investigation by Boomsma et al., (2003) revealed that the enhanced heat transfer comes at a high cost because the pressure drop increases significantly. They reported that brazing imperfections contributed to increased pressure drop. Some of the cells close to the plate would be filled entirely with brazing material as the porous is further compressed and the cells become smaller.

The heating of a foam-filled channel for electronic cooling applications was explored by Bastarows and the team (1998). Conductive thermal epoxy bonding and brazing of the metal foam to a heated plate were used in experimental method. The test results showed that the brazed metal foam prevailed upon heat removal in comparison to the epoxy-bonded samples. Nawaz et al., (2010) studied open-cell aluminum metal foam as a compact replacement for conventional fins in brazed aluminum heat exchangers. The authors displayed that metal foams have promising potential, especially in the targeted use of air-cooling systems. They pointed out that the bonding method is important as contact resistance can play a considerable role in non-brazed structures.

Guarino et al., (2017) investigated the influence of thermal contact resistance on aluminum foam. The authors used three different types of contacts between the metal foam and base plate: simple contact, brazed contact and grease paste contact. The results demonstrated that the brazed contact reduces the thermal contact resistance significantly compared to the simple contact. This reduction in thermal contact resistance increased the heat transfer coefficient by 80%, thus greatly enhancing the heat transfer performance. The joining of aluminum foam was studied previously by examining the microstructure and mechanical properties of brazed joints (Bangash et al., 2018).

Dixit & Gosh (2017) studied the prospective of employing open-cell metal foams in passive cryogenic radiators which work on the principle of dissipating heat through radiation. As radiation heat transfer is the only usable heating or cooling mode in vacuum outer space, these radiators are ideal for space applications. For space applications, the low weight of open-cell metal foam makes it highly desirable. A theoretical model was developed using conventional fin theory to determine radiation heat transfer from a finned foam surface. Due to high surface area, the porous metal permits a deeper penetration of the incident radiation thereby enhancing the heat transfer rate. The metal foams were able to provide radiative cooling ten times greater than that of solid fins in the case of the geometry under study.

Wang et al., (2019) investigated the heat transfer in finned Cu foam heat sinks subjected to jet impingement cooling. The effects of pore density (10,20, and 30 PPI) were systematically investigated. The experimental results revealed that inserting Cu foam as fins positively improves the thermal performance. In addition, the thermal performance of finned Cu foams with 20 PPI exceeds that of a conventional finned heat sink showing great potential to replace traditional heat sinks. However, this led to a larger pressure drop than conventional finned heat sink. It was concluded that finned Cu foams have a better heat transfer performance than conventional one with the same number of fins.

Porous metal foams exhibit significant potential in heat management applications due to the large surface area. Zhang et al., (2018) experimentally investigated a heat sink with porous Cu as conductive material for CPU cooling. The results show that cooling capacity of porous Cu increased with increasing inlet and outlet pressure difference. It was discovered that by replacing a microchannel heat sink with a porous Cu heat sink increases the heat sink coefficient by 28.5 %. Kiwan et al., (2020)

experimentally investigated natural convection heat transfer using porous fins attached to the outer surface of a vertical cylinder. The study showed a clear enhancement of heat transfer when porous fins are used. The minimum enhancement of heat transfer coefficient was 7.9 % when using one fin with a 10 mm thickness, and the maximum enhancement of heat transfer coefficient reached 131% when using porous layer.

Feng et al., (2018) experimentally investigated convection in metal foam heat sink. The test sample was made in-house by attaching several foam strips to Cu substrate. The experimental results revealed that there exists an optimum open slot width (5-8 mm) for maximum heat transfer coefficient. At the optimum open slot width, the heat transfer coefficient is enhanced by 14.9 %, 21.3 %, 37.6 % at the foam height of 10 mm, 20 mm and 40 mm, respectively. Zhong et al., (2020) designed micro-channel heat sinks based on different metal foams attached to Cu substrate. Among different micro-channel heat sinks, the heat dissipation of strap metal foam outperformed the cube and colum one. The enhanced forced convection resulted in an increase of heat transfer performance which was demonstrated by relevant experiments and numerical analysis. The experimental result was consistent with the numerical simulation. Therefore, the work put forward a strategy to optimize heat transfer performance of metal foam heat sink via forced convection.

The literature presented above indicates that different types of porous metals are being utilized in cooling devices. The joining of stainless steel and aluminum metal foams has also been studied previously in terms of the microstructural and mechanical properties of brazed joints (Shirzadi et al., 2004; Bangash et al., 2018). However, studies on the microstructure characterization and mechanical properties of joints brazed using porous Cu have not yet been reported in the literature. Brazing has been identified as the most suitable method of joining porous metal and substrate as it facilitates good

bonding between them and enhances heat transfer significantly (Sekulic et al., 2008). The successful joining of porous Cu to a Cu plate is substantial when considering porous Cu in the design of cooling devices such as heat exchangers.

2.6 Summary

The literature presented above enhanced the knowledge required to set up the methodology presented in the next chapter. Firstly, the materials required to conduct the experiment were studied and their properties were evaluated. Porous Cu is known to have many interesting combinations of physical and mechanical properties reported in the literature. The amorphous filler metal known as MBF 2005 was used to join the porous Cu to Cu substrate. The main advantage of this filler metal is low liquidus temperature which allows brazing to be performed at lower temperature.

Furnace brazing will be employed for joining of materials due to its adaptability to mass production. It is a semi-automatic process used widely in industrial operations. The advantage of using brazing over other metal-joining techniques is its ability to braze complex and multi-part assemblies cost effectively. The effects of brazing temperature and time were studied extensively in literature to understand their effects on microstructure and mechanical properties. It is widely acknowledged that these parameters play a vital role in successful brazing methods. Finally, the applications of porous copper were studied to understand their role in heat management devices and find the bottlenecks that are preventing this new generation of materials from reaching its potential.

CHAPTER 3: METHODOLOGY

This chapter describes all the experimental procedure involved in this research and previous literature related to the experiment. It mainly describes the type of materials, measurements, machines and set up parameters required for the experiment.

3.1 Materials

Pure solid 99.9 (wt. %) Cu plate in the size 500 x 500 x 3 mm^3 was purchased from C&W Hardware Sdn. Bhd. A piece of amorphous filler metal known as MBF 2005 was purchased from Metglass, Inc in size 40 x 125 mm^2. The filler composition was Cu-9.7Sn-5.7Ni-7P (wt.%) and had a 50μm thickness. Pure porous copper 99.9 (wt. %) with 15 PPI was purchased from Duranice Applied Materials in size 50 x 64 x 5 mm^3. Silicon carbide (SiC) abrasive paper was manufactured by Struers, USA. The alumina micro polish of 0.05 micron used to ground Cu was manufactured by Buehler, USA.

3.2 Sample Preparation

In this research, a pure solid 99.9 (wt.%) Cu plate available commercially and 15 PPI pure porous Cu were cut using an Electrical Discharge Machining (EDM) wire cutter into 15 x 15 x 3 mm^3 and 10 x 10 x 5 mm^3 dimensions, respectively. A piece of Cu-based filler metal known as MBF 2005 (from Metglass, Inc) with Cu-9.7Sn-5.7Ni-7P (wt.%) composition and 50μm thickness produced using rapid solidification was prepared in an approximate size of 13 x 13 mm^2. The solidus and liquidus temperatures of the filler metal are 591 ºC and 643 ºC, respectively (Table 3.1). Several advantages, such as extremely high chemical and phase homogeneity, higher diffusivity, narrow melting, and solidification ranges have been reported for this amorphous filler metal.

Table 3.1: Chemical composition and characteristic of filler metal working temperature

Filler metal	Chemical composition (mass %)				Solidus Temperature (°C)	Liquidus Temperature (°C)
MBF2005	Cu	Ni	Sn	P	591	643
	77.6	5.7	9.7	7.0		

Figure 3.1 and Figure 3.2 show the materials cut using EDM wire cutter. Prior to brazing, the solid Cu surface was scrubbed with 800 grit SiC paper and the roughness was measured to be 0.16. The porous Cu was immersed in a diluted solution of 5ml sulfuric acid and 95 ml distilled water to obtain a clean, oxide-free surface. After the materials were cleaned and dried, they were arranged layer by layer in a clamp system. Solid Cu is put at the bottom, followed by filler metal, porous Cu and solid Cu on the top side forming a sandwich configuration. Figure 3.3 illustrates the arrangement of the sample assembled in the clamp system. The sample was inserted into the furnace together with the clamp system to ensure all layers stay intact while brazing.

Figure 3.1: Materials cut using EDM wire-cutter; porous Cu

Figure 3.2: Materials cut using EDM wire-cutter; solid Cu

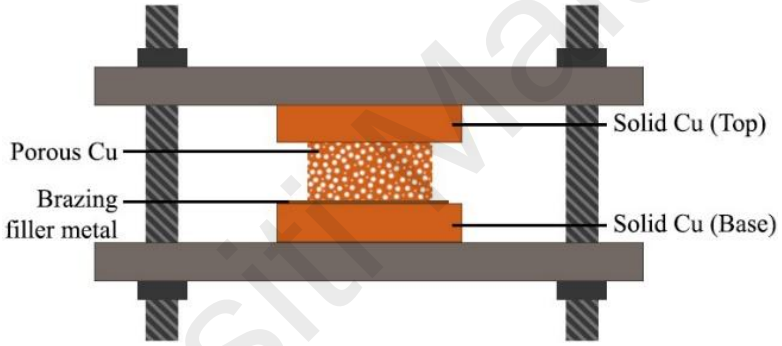

Figure 3.3: Schematic illustration of specimen arrangement in a clamp system

3.3 Brazing Process

The brazing furnace used in this research is a KYK tube furnace as shown in Figure 3.4. It uses argon gas to produce a protective atmosphere and prevent oxidation of sample. Firstly, the sample is inserted in center of the tube. By using a cylindrical rod, the sample is pushed inside the tube until it reaches the center. Then, the tube is tightly closed. The program is set according to the required temperature and holding time in the heating controller. After the program is ready, the cooler (water) and argon gas with constant flow rate of 3.5 L/min is turned on. Lastly, the run button is pressed which starts the program. When the program is finished, the sample is allowed to cool before removing it from the tube.

Figure 3.4: KYK tube furnace

3.3.1 Sample Brazing Temperatures and Holding Times

In this research, brazing temperature and holding time are the main parameters that need to be observed. The setup temperatures are 660 ˚C, 680 ˚C and 700 ˚C. Each temperature undergoes three different holding times which are 5, 10 and 15 minutes. Figures 3.5-3.7 below illustrates the arrangement of the samples according to the specific temperature and time.

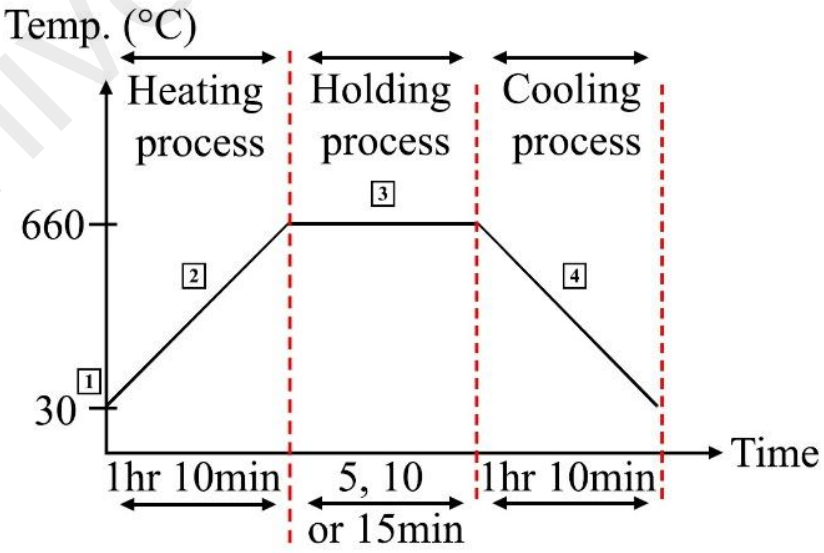

Figure 3.5: Brazing profile of sample with the setup temperature of 660 ºC

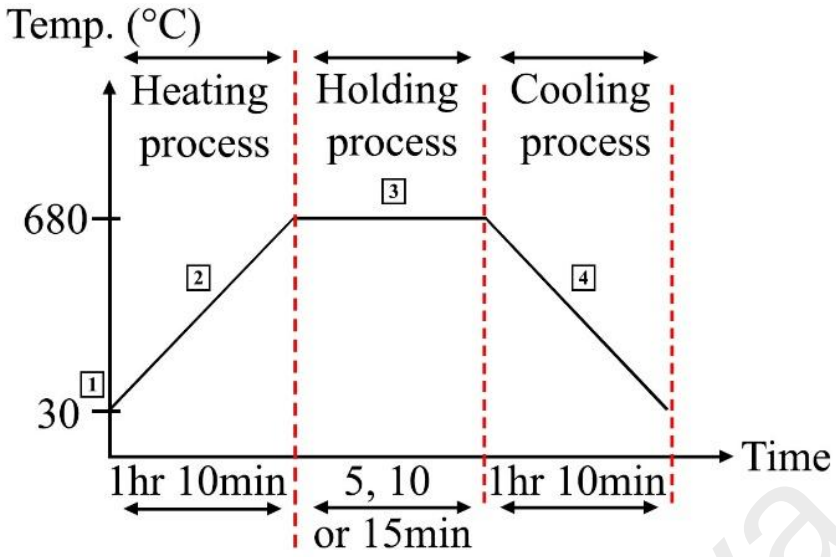

Figure 3.6: Brazing profile of sample with the setup temperature of 680 ºC

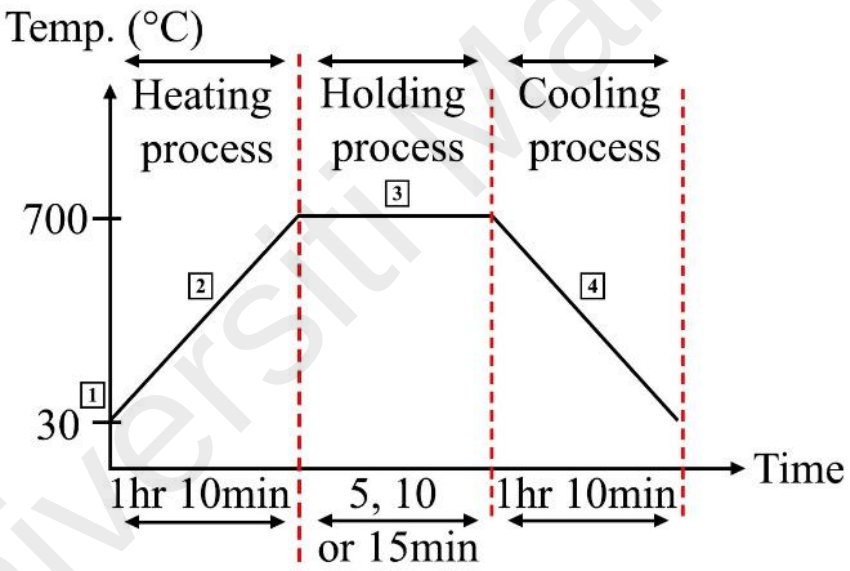

Figure 3.7: Brazing profile of sample with the setup temperature of 700 ºC

As mentioned earlier, the program must be set according to required temperature and time. To fulfill that requirement, the program is based on 4 segments as shown in figures 3.5-3.7. For segment 1, the temperature is set to 30 ºC. The initial temperature in the tube furnace will rise to 30 ºC before the heating process is started. The heating process starts in segment 2 where the temperature will increase from 30 ˚C to the required temperature (660 ˚C, 680 ˚C and 700 ˚C). When the heating temperature reaches the required temperature, it will hold for some time (5, 10 and 15 minutes).

Segment 3 represents the holding time for each sample. After the holding time is completed, the temperature will decrease to room temperature. The cooling stage is in segment 4. For the brazing process, the average heating and cooling rates were set at 10 ºC /min (Jattakul & Kanlayasiri, 2018). Hence, for complete brazing process there are 3 main steps which are pre-heating, heating, holding, and cooling.

3.4 Microstructural Evaluation of Brazed Joints

The microstructure of brazed joints was evaluated using characterization equipment such as SEM-EDS and X-ray diffraction.

3.4.1 SEM-EDS Analysis Method

After brazing is completed, the sample needs to be mount so it is easier to grip while cutting, grinding and polishing. To observe the microstructure, all the samples require grinding and polishing. The samples were ground using various abrasive SiC ranging from 300-2400 grit. After grinding, the samples were polished to a mirror finish using 0.5 µm alumina suspension micro polish. In order to observe the joint interface details, the microstructural characterization was conducted using a Scanning Electron Microscope (SEM) model Phenom Pro X Desktop equipped with an Electron Dispersive X-ray Spectrometer (EDS).

Scanning electron microscopy equipped with energy dispersive spectroscopy (SEM/EDS) is the best known and most widely used of the surface analytical techniques for microstructural characterization. The number and energy of the X-rays emitted from a specimen can be measured by an energy-dispersive spectrometer. As the energies of the X-rays are characteristic of the difference in energy between the two shells and of the atomic structure of the emitting element, EDS allows the elemental composition of the specimen to be measured. There are several methods when applying EDS in the experiment depending on what kind of outcome such as mapping, point analysis, area

analysis, etc. is required. In this experiment, EDS points analysis was used to identify the filler metal elements at joint interface. EDS mapping was also performed to analyse the concentration of filler elements.

3.4.2 X-RAY Diffraction Analysis

In order to obtain information about the structure of crystalline materials, X-ray diffraction (XRD) relies on the dual wave/particle nature of X-rays. The identification and characterization of compounds based on their diffraction pattern is a primary application of the technique. An X-Ray Diffractometer (XRD) model PANalytical Empyrean was employed for testing and analysis using HighScore software to determine the molecular structure in the 2θ range of 5 – 99 °. A continuous scan type was used with a step size of 0.02 ° and scan step time of 148 seconds. XRD helped to identify the different phase compounds formed at the interface.

3.5 Evaluation of Mechanical Properties

The mechanical properties were evaluated after brazing by performing Vickers microhardness test and compression test on various parameters.

3.5.1 Vickers Micro-Hardness Test

The Vickers hardness test method consists of indenting the test material with a diamond indenter, in the form of a pyramid with a square base and between opposite faces subjected to a test force of between 1gf and 100kgf. The full load is normally applied for 10 to 15 seconds. Vickers microhardness test analysis was carried out to determine the hardness of the joint interface and porous Cu after brazing. The test analysis was carried out under a test force of 980.7mN for duration of 5 seconds. The microhardness tester model used was HMV 2T E, Shimadzu. The sample was indented at several points of brazed joint interface and porous Cu surface. Figure 3.8 shows the

microhardness indents made at base joint, porous copper and top joint interface. The hardness values were recorded, and the data saved for analysis.

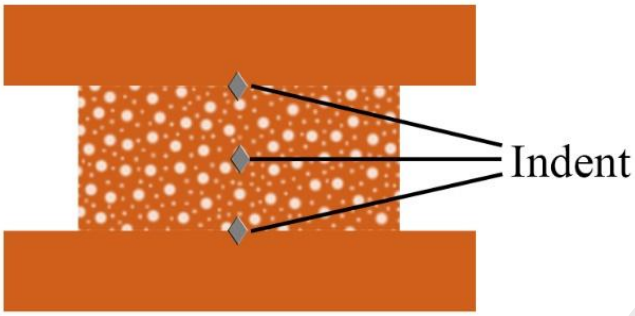

Figure 3.8: Schematic illustration of microhardness indent

3.5.2 Compression Test

The brazed samples were subjected to compression by an Instron Universal Testing Machine (Model 3369). The software used for the test was Instron Bluehill 2.0. Several initial parameters were set, and a separate profile was created for the sample due to its square shape. The crosshead speed of the mounted jig was set to 0.25 mm/min. After setup, a porous Cu sample before brazing was compressed for comparison. Then, different samples brazed at varying parameters were compressed to observe the changes after brazing. The samples had an initial thickness of 5 mm and final thickness of 2 mm. A tolerance of 2 mm was left to ensure the Cu plates attached to porous Cu do not affect the compression test results of porous Cu. A similar technique was used by Zahri et al., (2019) where different PPI foams were brazed and compared to nonbrazed Cu foam. It is significant to perform compression test on brazed samples to evaluate the rigidity of porous copper during service. Due to the long service life, the rigidity of porous Cu is important when considering it in cooling devices such as heat sink or heat exchanger.

CHAPTER 4: RESULTS & DISCUSSION

This chapter represents the results and discussion obtained from the experiment. All the findings and data gathered from the experiment are discussed thoroughly in this chapter. The results are presented in the form of images, tables, and graphs.

4.1 Effects of Brazing Parameters on the Microstructure of the Brazed Joints

The effects of brazing temperature and time are evaluated using microstructure characterization techniques. The data obtained for several different parameters is presented and compared for analysis.

4.1.1 Scanning Electron Microscopy (SEM) and Energy Dispersive Spectrometer (EDS) Analysis for all Parameters

The microstructure characterization was done using SEM/EDS to examine the intermetallic compounds that formed at the joint interfaces. The brazing filler metal placed at the base diffused into porous copper during brazing, and the filler metal joined the base and top side. In order to identify the spread of the filler alloy, EDS point analysis is used at brazed joint interface on both sides of porous Cu.

A. Sample 660 ºC, 5 min

Figure 4.1 illustrates the scanning image of base and top joint of sample at 660 ºC, 5 min holding time. The magnifications are 530x and 480x. The visibility of microstructure in dark grey is clear at the base joint.

To identify the existing filler elements, EDS point analysis results from points marked in Figure 4.1 are presented in Table 4.1.

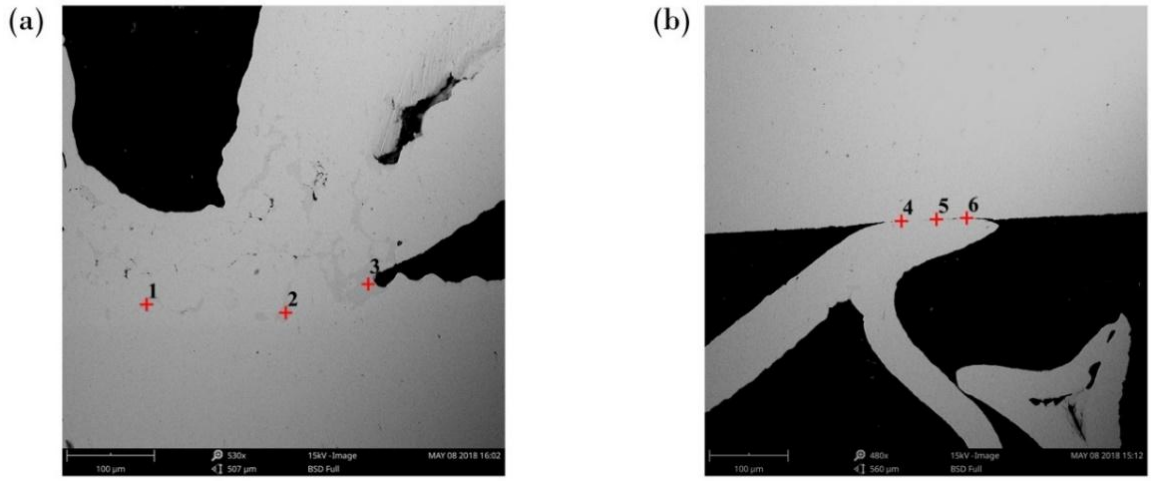

Figure 4.1: SEM images for 660 ºC, 5 min with marked points for EDS analysis for; (a) base of joint, and (b) top of joint

Table 4.1: EDS composition (at. %) at different points marked in Fig. 4.1

Point	BASE OF JOINT			TOP OF JOINT		
	1	2	3	4	5	6
Cu	88.75	61.61	78.24	98.75	99.62	98.35
P	6.11	20.90	19.23	0.92	0.77	0.32
Ni	2.79	17.03	1.52	-	-	0.76
Sn	2.34	0.46	1.01	0.35	-	0.57

The porous Cu joined to the base Cu plate displays a clearly visible diffusion of filler metal elements at the joint interface in dark grey. The dark grey areas indicate interfacial interaction between Cu and molten filler, involving dissolution, diffusion, and chemical reactions during the brazing process. The main elements forming the dark grey microstructure at base of joint are P and Ni mainly present at point 2 and 3 in Table 4.1. However, Micro-voids and cracks were identified at the base joint interface, leading to doubts about the joint's efficiency at low brazing temperature and time. Furthermore, the filler alloy was unable to diffuse to the top side as negligible amount of filler elements were detected in points 4, 5 and 6 in Table 4.1.

B. Sample 660 ºC, 10 min

To identify the existing filler elements, EDS point analysis results from points marked in Figure 4.2 are presented in Table 4.2.

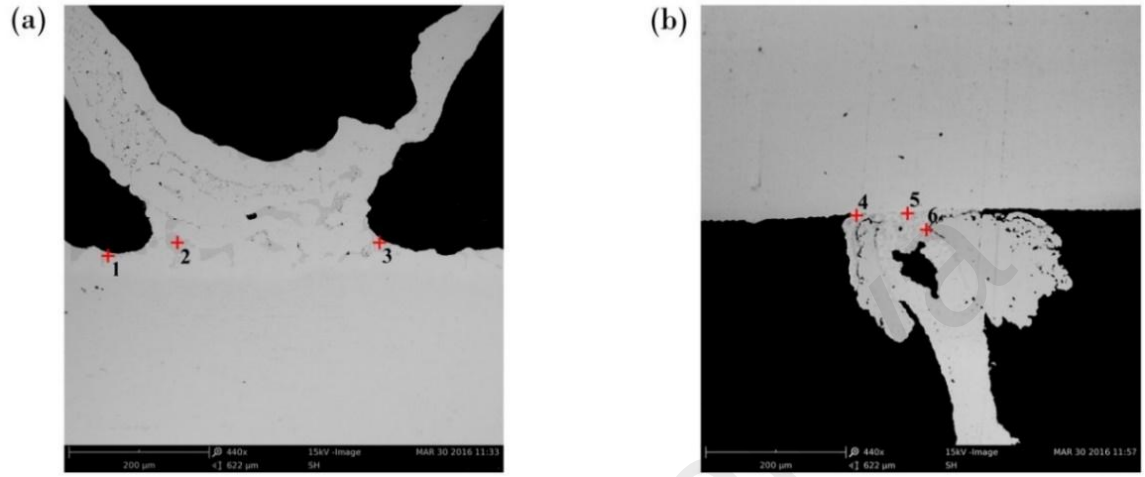

Figure 4.2: SEM images for 660 ºC, 10 min with marked points for EDS analysis for; (a) base of joint, and (b) top of joint

Table 4.2: EDS composition (at. %) at different points marked in Fig. 4.2

Point	BASE OF JOINT			TOP OF JOINT		
	1	2	3	4	5	6
Cu	76.8	82.7	42.1	48.9	75.1	44.0
P	23.2	17.1	15.9	12.0	7.1	14.6
Ni	-	-	42.0	38.2	16.7	40.9
Sn	-	0.3	0.0	1.0	1.1	0.5

Figure 4.2 (a) and 4.2 (b) illustrate the cross section of the top and base of the joint brazed at 660 ºC for 10 min. At higher holding time, the diffusion of filler alloy at the base side is prominent. According to marked points 1, 2 and 3 at the base side, P is the main element in the dark grey region leading the formation of microstructure. Ni was only detected at point 3 on the base side towards the corner of joint interface. However, high amount of Ni was detected at the top of joint in points marked as 4, 5 and 6. This suggests that at higher holding time, diffusion of Ni towards joint interface improves rapidly. This will lead to better joint formation as Ni increases strength of the joint

(Hissyam et al., 2017). However, micro-voids and cracks were detected on top and base side of the joint. The reason for this shortcoming is that at lower holding time and temperature, the filler was unable to completely react with Cu.

C. Sample 660 ºC, 15 min

To elucidate the atomic behavior at the brazed joint interfaces, the distribution of existing filler metal elements was measured by EDS. Figure 4.3 (a) and 4.3 (b) illustrate cross sections of the top and base of the joint brazed at 660 ºC for 15 min. The interfacial microstructure of the major elements at each spot marked in Figure 4.3 (a) and 4.3 (b) detected by EDS are tabulated in Table 4.3.

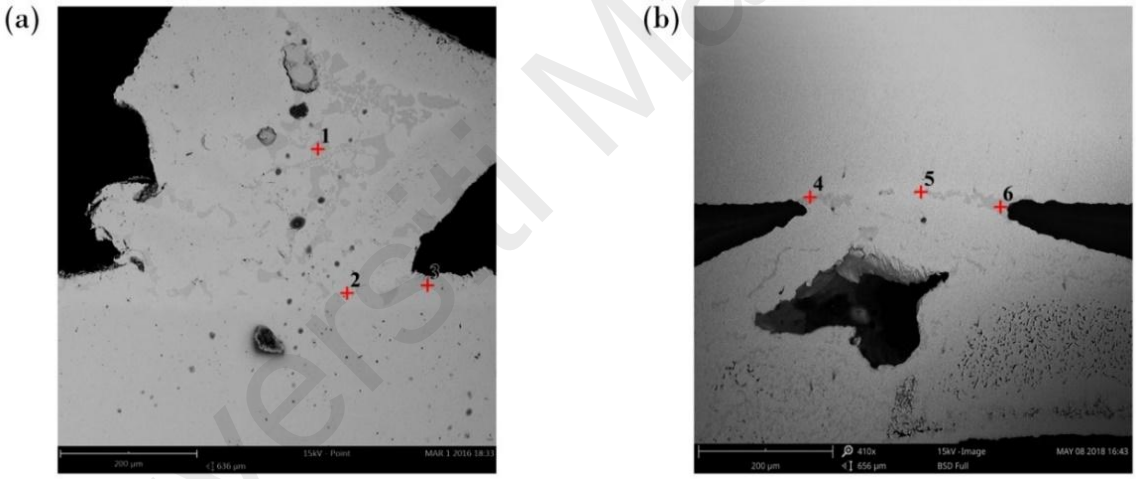

Figure 4.3: SEM images for 660 ºC, 15 min with marked points for EDS analysis for; (a) base of joint, and (b) top of joint

Table 4.3: EDS composition (at. %) at different points marked in Fig. 4.3

Point	BASE OF JOINT			TOP OF JOINT		
	1	2	3	4	5	6
Cu	78.4	89.1	65.7	71.22	61.26	76.74
P	20.0	6.5	7.9	24.46	23.36	19.12
Ni	0.9	1.5	25.2	4.33	15.18	3.67
Sn	0.6	2.9	1.1	-	0.19	0.47

It shows that the base contained a considerable amount of phosphorus (P) distributed across the joint interface and porous Cu area. The EDS analysis of the base of the joint at point 1 shows that the dark region contained Cu (78.4 at %), P (20.0 at %) and small amounts of Nickel (Ni) and Tin (Sn), which indicates a Cu solid solution with a Cu-P phase according to the Cu-P phase diagram (Predel, 1994). A substantial amount of Ni was identified at point 3. Based on the EDS results in Table 1 for the top joint interface, the region marked as point 5 was enriched with Cu (61.26 at. %), P (23.36 at. %), Ni (15.18 at. %) and Sn (0.19 at %), signifying possible phases of Cu-P and Cu-Ni.

There were high percentages of P element at all points marked on the top joint interface in Table 4.3. Therefore, it appears that P was the main element contributing to the formation of the dark grey area. Element P in the filler metal had the function of accelerating the dissolution of Cu during brazing (Rupert, 1996). However, the Ni content was very low except at point 5, indicating that Ni was diffusing slowly compared with P. A successfully brazed joint was achieved with all parameters tested at the base side. However, the top side had cracks at lower brazing temperature of 660 ºC due to insufficient diffusion of filler metal to the top side. The reaction product at the base joint is thick due to the high presence of filler elements, while the top joint has a thin and loose arrangement. It is perceived that the reaction product was thinner at the base, flowing towards the porous copper and the top joint after increasing holding time.

D. Sample 680 ºC, 5 min

Figure 4.4 (a) and 4.4 (b) illustrate cross sections of the top and base of the joint brazed at 680 °C for 5 min. To identify the elements present, EDS point analysis was carried out and the results are shown in Table 4.4.

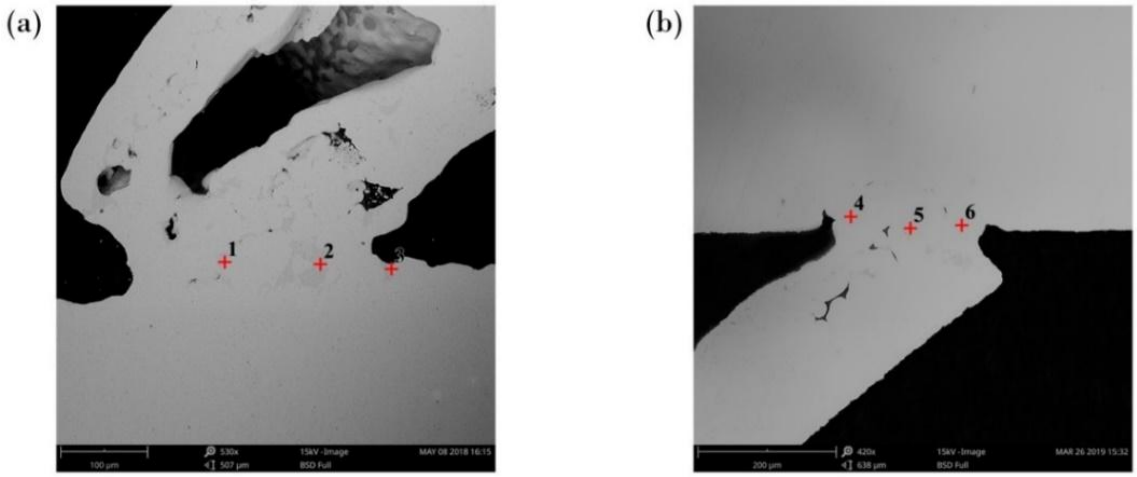

Figure 4.4: SEM images for 680 ºC, 5 min with marked points for EDS analysis for; (a) base of joint, and (b) top of joint

Table 4.4: EDS composition (at. %) at different points marked in Fig. 4.4

Point	BASE OF JOINT			TOP OF JOINT		
	1	2	3	4	5	6
Cu	75.74	76.65	78.04	97.39	51.02	97.17
P	23.54	21.87	20.54	1.55	26.14	1.69
Ni	-	1.48	1.42	0.56	-	0.47
Sn	0.72	-	-	0.50	22.84	0.67

The EDS analysis at base side of joint shows higher percentage of P element at all three points. Again, small amounts of Ni were detected at lower holding time of 5 min. Therefore, it is evident that at low holding time, Ni was unable to diffuse into the joint interface on both sides. Table 4.4 revealed higher percentages of P and Sn elements at top side of joint. Point 5 was enriched with Cu (51.02 at. %), P (26.14 at. %), and Sn (22.84 at. %), signifying possible phases of Cu-P and Cu-Sn. By increasing the brazing temperature, voids and cracks can be minimized. However, the diffusion of filler elements at lower holding time is not significant as the top joint strength would be compromised with low Ni content. It can be observed from figure 4.4 that the base joint is devoid of imperfections. However, at low holding time of 5 min, the filler elements are unable to diffuse completely towards top joint interface.

E. Sample 680 ºC, 10 min

To analyze the role of brazing time in microstructure formation, the EDS results for the sample brazed at 680 ºC for 10 min (Figure 4.5) are presented in Table 4.5.

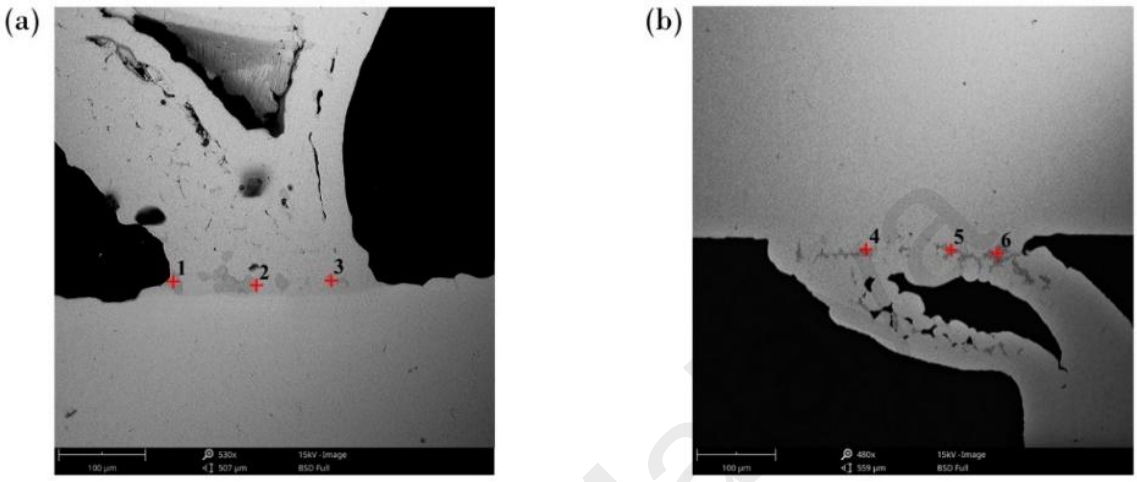

Figure 4.5: SEM images for 680 ºC, 10 min with marked points for EDS analysis for; (a) base of joint, and (b) top of joint

Table 4.5: EDS composition (at. %) at different points marked in Fig. 4.5

Point	BASE OF JOINT			TOP OF JOINT		
	1	2	3	4	5	6
Cu	75.90	76.87	84.04	39.82	45.42	68.16
P	21.86	21.06	13.71	21.02	18.36	11.56
Ni	1.65	1.54	1.12	38.87	35.81	19.84
Sn	0.59	0.52	1.13	0.29	0.41	0.44

The grey region marked as point 3 in Table 4.5 was enriched with Cu (84.04 at %), P (13.71 at %), Ni (1.12 at %) and Sn (1.13 at %). Point 3 apparently consisted of Cu solid solution and Cu-P phase compounds (Miettinen, 2001). However, there was a lower percentage of Ni element at the base compared to the sample brazed at 660 ºC. At a high temperature, better diffusion of Ni from the filler metal through the porous Cu and top joint interface was noted (in line with the high values in Table 4.5 for the top of the joint). The EDS analysis of the brazed top joint interface shows that the dark region at point 5 was composed of Cu (45.42 at %), P (18.36 at %), Ni (35.81 at %) and a

negligible amount of tin. This dark phase apparently consists of Cu-P and Cu-Ni phase compounds. The diffusion of filler metal into the top of the joint improved with temperature and time due to the inter-diffusion of Ni towards the porous Cu and top joint area. The homogenous filler spread through capillary action by penetrating the clearances between Cu. Figure 4.5 signifies that the thickness of the reaction interface reduced at the base, diffusing into the porous Cu and top of the joint.

F. Sample 680 ºC, 15 min

Figure 4.6 (a) and (b) illustrate cross sections of the top and base joint brazed at 680 ºC, 15 min. To identify the elements present, EDS point analysis results are shown in Table 4.6.

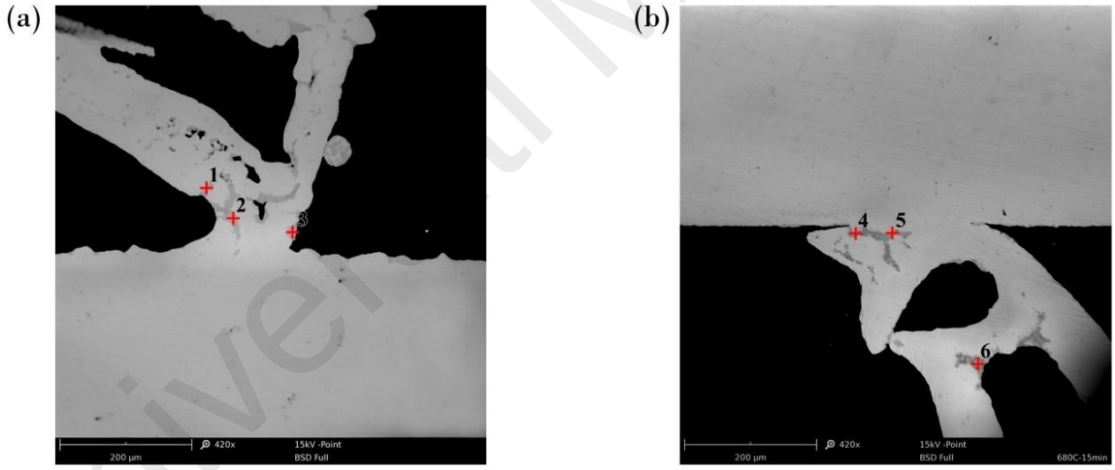

Figure 4.6: SEM images for 680 ºC, 15 min with marked points for EDS analysis for; (a) base of joint, and (b) top of joint

Table 4.6: EDS composition (at. %) at different points marked in Fig. 4.6

Point	BASE OF JOINT			TOP OF JOINT		
	1	2	3	4	5	6
Cu	76.6	77.0	59.7	40.9	34.2	42.6
P	22.2	22.3	33.0	21.9	24.1	20.5
Ni	0.9	0.4	0.6	37.2	41.6	36.9
Sn	0.3	0.2	6.7	-	0.2	-

This analysis revealed that phosphorus (P) and nickel (Ni) were the main elements contributing to the microstructure formation. The joint interface was mainly composed of Cu solid solution and possibly a Cu-P phase at the base of joint (Predel, 1994). It was noted that the amount of Cu-P phase region at the joint interface increases with temperature due to higher diffusion of filler metal elements. A higher composition of Ni content was noticed in the top side of joint, thereby increasing the reaction products formed at the top joint interface. The top joint marked as point 5 consisted of P (24.1 at. %), Cu (34.2 at. %) and Ni (41.6 at. %). This indicates possible Cu-Ni and Cu-P phases at the brazed joint interface. The diffusion of filler metal into the top of the joint improved with temperature and higher holding time.

The filler spread through capillary action by penetrating the clearances between Cu. The dark grey residual product of the filler metal seemingly diffused from the base joint interface into the porous Cu and top joint area by increasing the brazing temperature to 680 ºC and holding time to 15 min. Figure 4.6 suggests that the interdiffusion and interaction between the filler metal and Cu increased significantly. The EDS results obtained are in good agreement with previous studies on pure solid Cu joints brazed with a similar amorphous filler metal (Jattakul & Kanlayasiri, 2018; Zhang et. al., 2016). The studies were performed using same filler elements and the brazing parameters were similar aswell. However, the only difference is that the studies are based on solid Cu joints.

G. Sample 700 ºC, 5 min

The cross sections of the brazed specimen at 700 ºC, 5 minutes was examined using SEM with EDS point analysis to study the element distributions shown in Table 4.7.

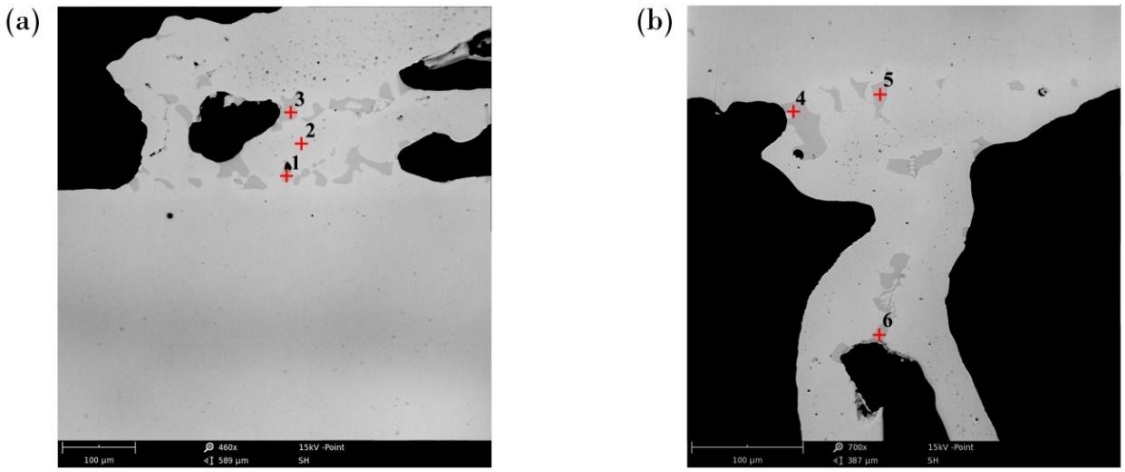

Figure 4.7: SEM images for 700 ºC, 5 min with marked points for EDS analysis for; (a) base of joint, and (b) top of joint

Table 4.7: EDS composition (at. %) at different points marked in Fig. 4.7

	BASE OF JOINT			TOP OF JOINT		
Point	**1**	**2**	**3**	**4**	**5**	**6**
Cu	74.0	92.5	73.9	76.4	72.7	71.3
P	19.6	1.9	20.7	20.9	20.5	21.9
Ni	-	-	-	-	-	-
Sn	-	-	-	-	-	-

Based on the EDS results tabulated in Table 4.7, P concentration was high at most spots in the dark grey region. Therefore, the dark grey region was mainly composed of P at 700 ºC, 5 min holding time. The top and base joint interface was mainly composed of Cu solid solution and Cu-P phase according to Cu-P phase diagram (Predel, 1994). Ni was not detected at this parameter which is like the trend observed at lower temperatures of 680 ºC, and 660 ºC for 5 min holding time. A residue of filler metal was observed for each sample at low holding time of 5 min after the brazing experiment. However, as the brazing temperature is higher compared to other two parameters at low holding time, complete joints were formed at the base and top side as shown in Figure 4.7 (a-b). Therefore, it can be concluded that brazing temperature plays a crucial role in formations of joints.

H. Sample 700 ºC, 10 min

Figure 4.8 shows the cross sections of the base and top joint at 700°C for 10 min marked with points at which EDS point analysis was performed to further evaluate the microstructure. The major elements at each spot in Figure 4.8 detected by EDS are listed in Table 4.8.

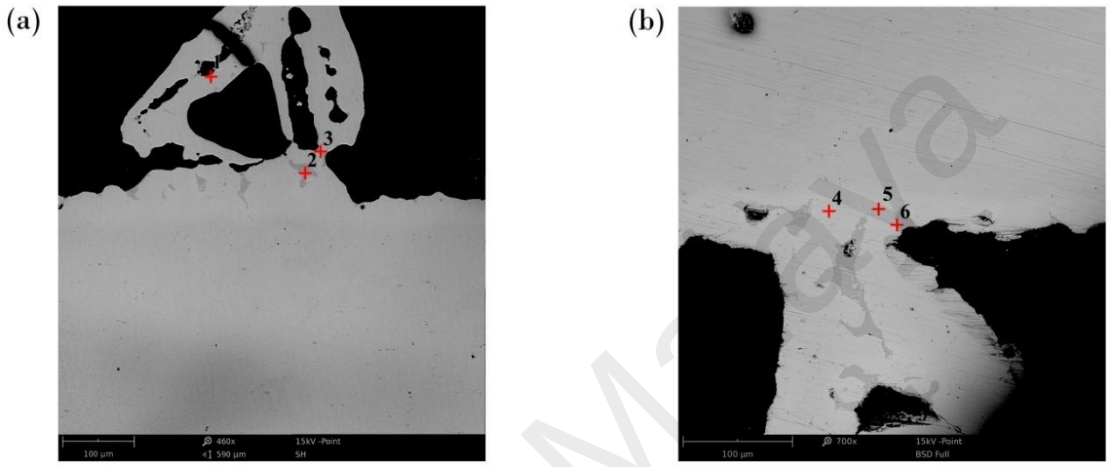

Figure 4.8: SEM images for 700 ºC, 10 min with marked points for EDS analysis for; (a) base of joint, and (b) top of joint

Table 4.8: EDS composition (at. %) at different points marked in Fig. 4.8

Point	BASE OF JOINT			TOP OF JOINT		
	1	2	3	4	5	6
Cu	78.5	74.6	71.7	77.2	72.0	75.5
P	12.2	17.4	21.3	21.8	26.9	13.7
Ni	7.9	7.6	5.1	0.8	0.9	8.2
Sn	1.4	0.4	1.9	0.2	0.2	2.6

Based on the EDS results tabulated in Table 4.8, the dark grey spot marked as point 2 was enriched with P (17.4 at. %), Cu (74.6 at. %), Ni (7.6 at. %) and Sn (0.4 at. %). The joint interface was mainly composed of Cu solid solution, Cu-P and possibly a Cu-Ni phase. There were high percentages of P at all points marked in Table 4.8 and considerable amounts of Ni were present at the base of joint. The spot marked as point 5 at the top joint interface was enriched with P (26.9 at. %), Cu (72.0 at. %) and small

amounts of Ni and tin (Sn). However, it is detected that the spot marked as point 6 had a high amount of Ni (8.2 at. %), which is towards the porous Cu area. Therefore, it should be highlighted that Ni was diffusing towards the top joint at a slower pace compared to P. However, there was a small quantity of Sn at all marked points. Furthermore, it is evident that the filler elements diffused into the porous Cu.

Sn as an active alloy and melting point depressant element diffused out of the filler metal towards the base metal and its concentration was low at the interface and center of the bond zone. Sn has a lower melting point and spread throughout the brazed joint according to which liquation occurred during brazing. Liquation in brazing is defined as the tendency of the lower melting constituents of the brazing filler metal to separate and flow away from the higher melting constituents upon heating (Kay, 2012).

I. Sample 700 ºC, 15 min

The EDS point analysis at 700 °C for 15 min shows the elemental distributions at the spots marked in Figure 4.9, which are tabulated in Table 4.9. The dark grey spot in the base joint marked as point 1 consisted of P (24.65 at. %), Cu (62.07 at. %) and Ni (13.28 at. %) indicating possible phases of Cu-P and Cu-Ni. There was a high percentage of P at all points tabulated in Table 4.9. However, no Ni was detected at points 2 and 3 due to the diffusion of Ni towards the porous Cu and top joint interface after increasing the holding time.

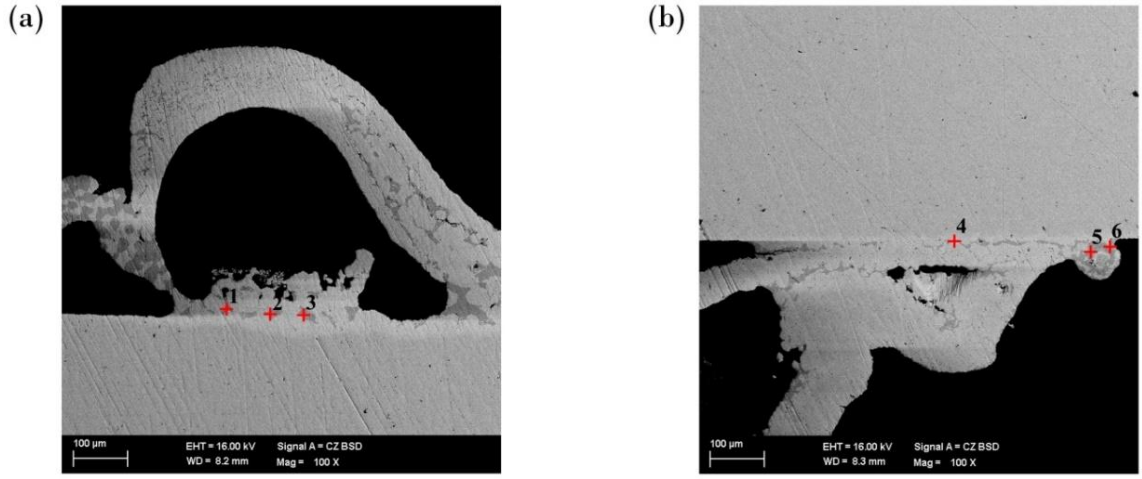

Figure 4.9: SEM images for 700 ºC, 15 min with marked points for EDS analysis for; (a) base of joint, and (b) top of joint

Table 4.9: EDS composition (at. %) at different points marked in Fig. 4.9

Point	BASE OF JOINT			TOP OF JOINT		
	1	2	3	4	5	6
Cu	62.07	72.21	71.09	57.81	28.19	55.20
P	24.65	27.79	28.91	24.23	28.20	16.20
Ni	13.28	-	-	13.28	43.61	28.60
Sn	-	-	-	-	-	-

The top joint marked as point 5 consisted of P (28.20 at. %), Cu (28.19 at. %) and Ni (43.61 at. %). This indicates possible Cu-Ni and Cu-P phases at the top joint interface. Furthermore, Sn diffused out of the filler metal into the base metal, which is why Sn was not detected at all marked points in Table 4.9. Owing to its lowing melting point, Sn diffused out of the filler and spread through the base metal. The EDS results are in good agreement with a study by Zhang et al. (2016) on pure Cu joints brazed with a similar filler metal.

It is known that phosphorus acts as a fluxing agent (Rupert, 1996). As phosphorus has a deoxidizing effect, Cu-P filler metals tend to be self-fluxing. The addition of a nominal phosphorus content (7 wt.%) had a slight effect by reducing the joint ductility, while the addition of some nickel and tin improved the glass forming ability during the filler metal manufacturing process (Jacobson & Humpston, 2005). The most commonly

used additive in copper-based brazing filler metal is phosphorus because it can reduce the filler's melting point efficiently in accordance to the Cu-P phase diagram (Predel, 1994). Moreover, phosphorus can also improve the wettability and spreading ability of the filler metal (Dahlgren, 1997). The filler metal has high corrosion and wear resistance due to the presence of Ni, Sn and P. Ni offers better toughness and strength at high and low temperatures. Ni is commonly used as a diffusion barrier between Cu and Sn to suppress the formation of Cu-Sn intermetallic compounds, which is not favorable, because the formation of this thick phase will lead to crack propagation (Ghosh et. al., 2017).

The filler elements diffused better at higher temperature and holding time, especially Nickel. It is also noted that the filler diffusion to the top joint improved with increasing holding time. The element Sn completely diffused from the filler metal into the Cu plate due to the low melting temperature; therefore, Sn had low values in the EDS analysis. The P-rich phase appeared at all EDS points tabulated. However, by increasing the holding time the dark grey region migrated towards the porous copper and top joint. Hence, increasing the brazing time caused the dark grey region to move and concentrate towards the top side of the brazed joint. However, Sn did not exhibit gray region formation at all holding times. This indicates that Sn was distributed well at all holding times.

4.1.2 EDS Mapping Analysis for Brazing Porous Copper to Copper

One parameter was selected to be discussed for the EDS mapping analysis. The EDS compositional maps in Figures 4.10 and 4.11 show the element distribution in the area selected on the joint interface brazed at 680 ºC for 10 min. The EDS maps reveal that the reaction interface mainly consisted of Cu, Ni and P. From the spatial distribution of the elements, the joint contained Cu-rich phases in the eutectic composition. Although a certain amount of P diffused into Cu, a large quantity of P was still distributed in the

residual reaction product. Thus, P was the main element that formed a continuous reaction phase and had a key role in the interfacial reaction. Moreover, a significant amount of Ni diffused towards the top joint reaction interface due to the higher temperature (Figure 4.11). Sn as an active alloy and melting point depressant element diffused through the base metal and had a low concentration at the joint interface (Figure 4.10 and 4.11). Because Sn has a lower melting point, it spread throughout the brazed joint such that liquation occurred during brazing.

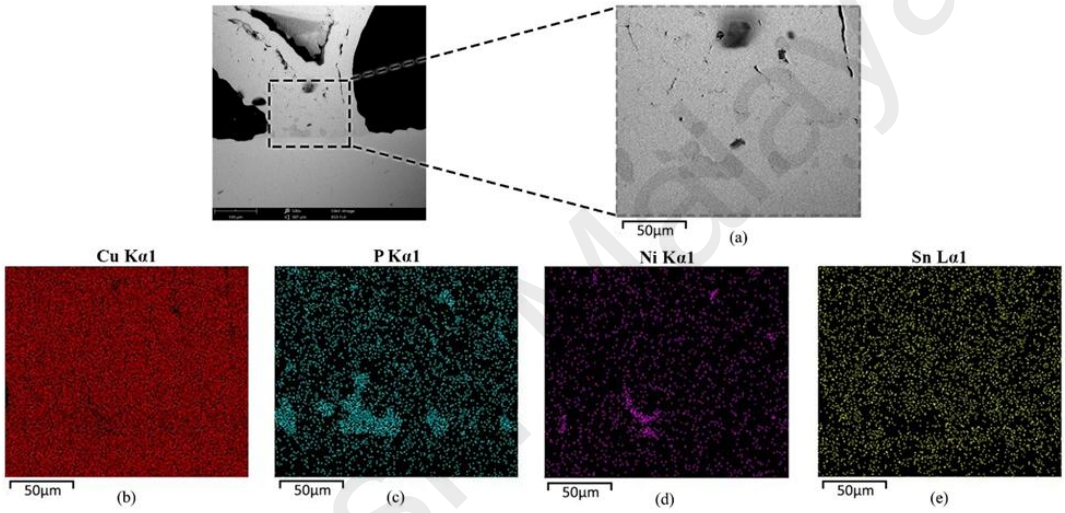

Figure 4.10: Map analysis of joint interface brazed at 680 ºC for 10 min: (a) SEM micrograph of the base of the joint; and elemental analysis of (b) Cu, (c) P, (d) Ni, (e) Sn

Figure 4.11 displays elemental maps of the top joint brazed at 680 °C for 10 min, which mainly consisted of Cu solid solution (Figure 4.11 (b)). It can be clearly seen that the joint consisted of two reaction layers which can be classified according to the difference in microscopic morphology. According to Figures 4.11 (c), certain amounts of P diffused into the base metal, but a large quantity of P was distributed mainly in the joint interface, forming the reaction product. A brittle Cu-P phase was produced during solidification according to the Cu-P-Sn system (Miettinen, 2003), which can certainly degrade the mechanical joint properties. Furthermore, Ni did not diffuse into the base metal completely and still existed as a reaction product at the joint interface forming a

Cu-Ni phase which can increase joint strength (Figure 4.11 (d)). According to the distribution of Sn in Figure 4.10 (e) and Figure 4.11 (e), it clearly shows that the reaction between Cu and Sn was very quick due to low melting point of Sn. Therefore, Sn was distributed well throughout the bonded region.

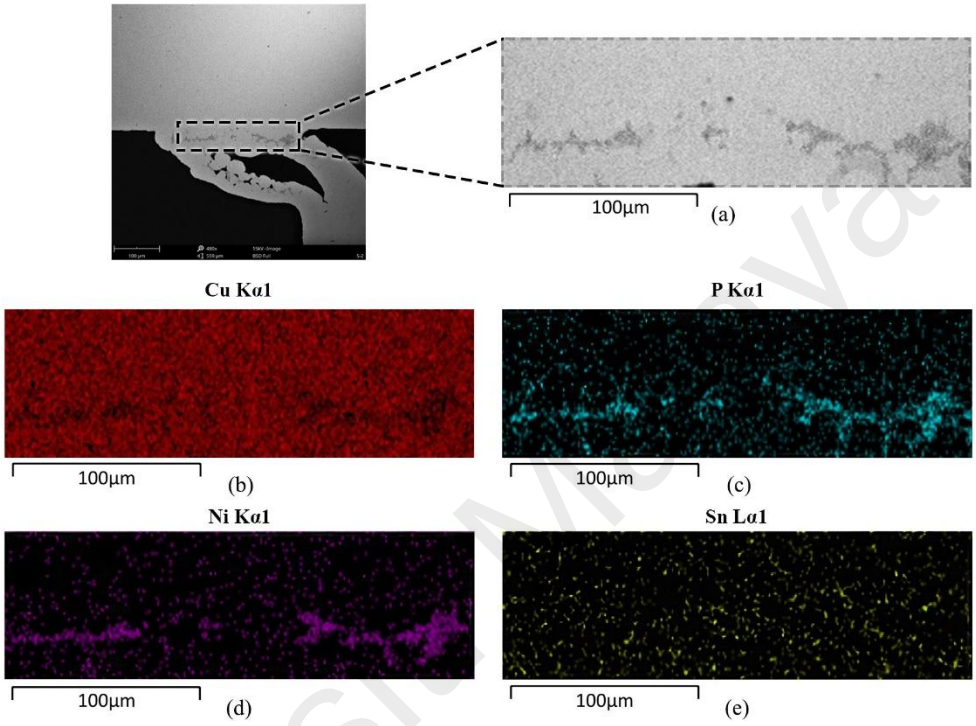

Figure 4.11: Map analysis of joint interface brazed at 680 ºC for 10 min: (a) SEM micrograph of the top of the joint; and element analysis of (b) Cu, (c) P, (d) Ni, (e) Sn

4.1.3 Temperature Effects on Microstructure of Porous Copper Surface

Figure 4.12 illustrates the microstructure formation at porous Cu surface after brazing at 660 ºC for 15 min. Filler has diffused from the base side into porous Cu clearly visible as the dark grey reaction product. The filler elements have mostly settled around the inside pore which is the weakest section in terms of strength. The EDS composition of points (1) – (4) in Figure 4.12 confirm that P is the main factor in the formation of the reaction product due to high values at all points. The region marked as Point 2 in Figure 4.12 was enriched with Cu (64.21 at %), P (20.94 at %), Ni (14.57 at %) and small amount of Sn, which indicates formation of Cu solid solution with Cu-P

phase according to the Cu-P phase diagram (Predel, 1994). The formation of Cu-P phase will lead to increase in rigidity of porous Cu. The region marked as point 4 consisted of Cu (38.84 at %), P (20.99 at %), Ni (40.05 at %) and small amount of Sn. This indicated formation of Cu-P and Cu-Ni phases which will lead to increase in strength of porous Cu. Also, higher amount of Ni seen in porous Cu which is placed at center confirms that diffusion of Ni element increases with holding time.

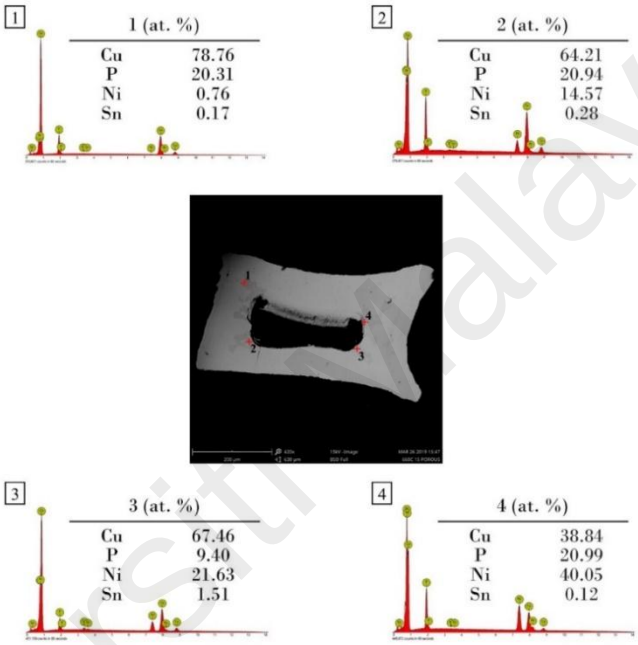

Figure 4.12: SEM micrographs with marked points (1) – (4), and EDS peak pattern with respect to points (1) – (4) of porous Cu brazed at 660 ºC for 15 min

Figure 4.13 illustrates the microstructure formation at porous Cu surface after brazing at 680 ºC for 15 min. It is evident that the filler metal has diffused into porous Cu from the base side creating the dark grey reaction product. The EDS composition of different points marked in Figure 4.13 confirms that P is the main factor in the formation of the reaction product as P diffused into porous Cu at points 1-4 which represent Cu solid solution matrix enriched with P. The region marked as Point 1 in Figure 4.13 was enriched with Cu (57.12 at %), P (19.24 at %), Ni (23.32 at %) and small amount of Sn, which indicates formation of Cu-P and Cu-Ni phases. However, excessive growth of brittle Cu_3P phase will give joints a low mechanical strength. This

finding has been revealed by Hasap et al., (2014) who stated that excessive formation of Cu_3P would encourage propagation of cracks and fractures. Furthermore, the behavior suggests that P has spread and settled in porous Cu. The spread was assisted by capillary action as molten filler diffused and coated the porous copper surface at an elevated temperature.

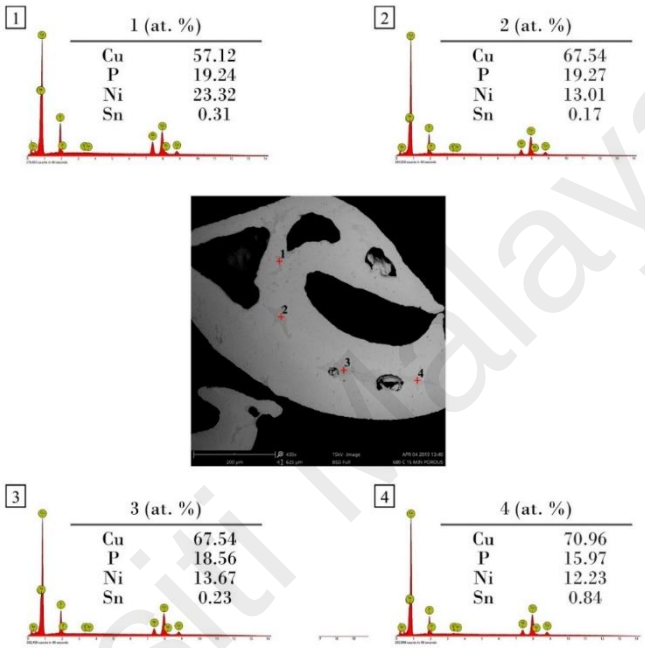

Figure 4.13: SEM micrographs with marked points (1) – (4), and EDS peak pattern with respect to points (1) – (4) of porous Cu brazed at 680 ºC for 15 min

Figure 4.14 illustrates the microstructure formation at porous Cu surface after brazing at 700 ºC for 15 min. The filler metal has diffused into porous Cu surface and settled around the edges of the pore creating the dark grey reaction product. The EDS composition of all points marked in Figure 4.14 again confirms that P is the main element responsible for the formation of dark grey reaction product. The region marked as Point 1 in Figure 4.14 was enriched with Cu (79.39 at %), P (19.15 at %), and small amounts of Ni and Sn, which indicates formation of Cu solid solution with Cu-P phase according to the Cu-P phase diagram (Predel, 1994). The Ni content at 700 ºC, 15 min is low due to its diffusion towards top joint interface. This reveals that due to increase in temperature, the diffusion of Ni towards top joint increases forming a joint with good

strength. Sn has diffused into the parent metal throughout the bonded region. The lower values of Sn observed in the EDS analysis support this observation. Overall, a considerable amount of reaction products formed at the porous Cu surface and largely the formation of Cu-P phase will harden the porous Cu and increase its strength. The filler metal successfully coated the porous Cu surface, resulting in an increase in hardness and strength, which will be discussed in the next sub-sections.

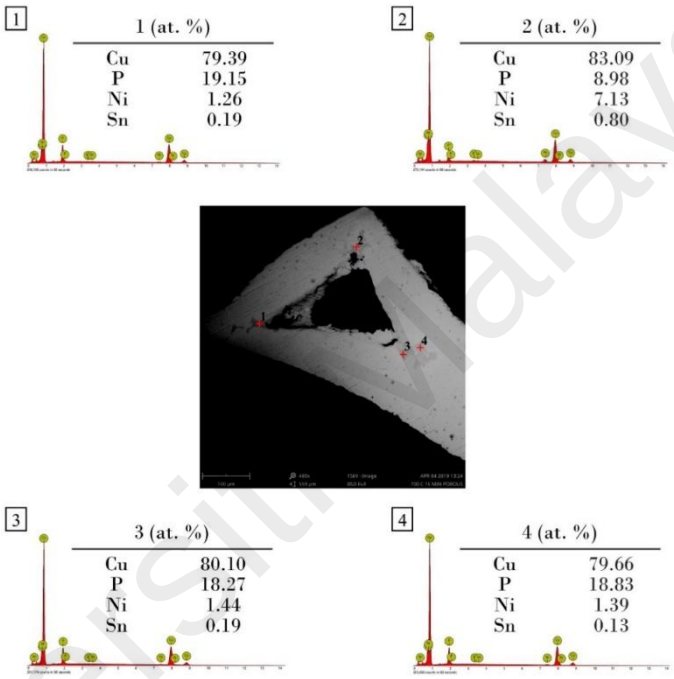

Figure 4.14: SEM micrographs with marked points (1) – (4), and EDS peak pattern with respect to points (1) - (4) of porous Cu brazed at 700 ºC for 15 min

4.1.4 Phase Identification of the Brazed Samples

XRD analysis was performed to confirm the results obtained from SEM microstructural analysis. It is noted that the joining of metals occurred after the filler metal wet the surface and reacted with the porous Cu/solid Cu. Although the brazing filler metal has four elements, Cu and Ni have the same crystal structure, similar radii, electronegativity, and valence. The Cu-Ni phase compound is an isomorphous system. Therefore, complete solubility occurs between them. As Cu and Ni exhibit complete solubility, the four-element filler alloy can be simplified to a Cu-Sn-P ternary alloy.

From the Cu-Sn-P system described by Miettinen (2003), the interaction of fillers at the brazed joint microstructure can be described by the endothermic reaction that has two stages:

$$Fcc + Bcc + Cu - P \rightarrow L + Fcc + Cu - P \quad \textbf{(4.1)}$$

$$L + Fcc + Cu - P \rightarrow L \quad \textbf{(4.2)}$$

As the brazing temperature exceeds the solidus temperature of the filler metal, the eutectic microstructure completely melts, and liquid phase occurs. The increase in temperature generates more liquid phase that migrates towards the filler metal surface. If an abundant liquid phase is generated inside the filler metal, dissolution across the base metal is faster and a liquid phase network forms in the braze seam. The liquid phase starts to flow towards the base metal surface under surface tension, rapidly reducing the filler metal thickness. The liquid phase interacts with the base metal in the form of the dissolution and diffusion of filler elements. In the subsequent cooling process, the liquid phase solidifies inside the brazed seams.

The XRD analysis was performed at three different parameters of 660 ºC, 680 ºC and 700 ºC for 15 min holding time. These parameters were prepared for different parts of one sample, including the base and top side with compressed porous Cu. All the samples analyzed exhibited a similar pattern of peaks, which appeared to indicate the formation of identical phases shown in Figures 4.15 – 4.17. It was revealed that all sharp peaks are related to Cu except Ni-Sn phase. As Ni has good wetting characteristics with Sn (Liu, et al., 2012), it seems to impart a greater degree of fluidity, allowing the metal to flow freely. Moreover, adding Sn as an alloying element lowers the filler metal melting temperature (Cui, et. al., 2014).

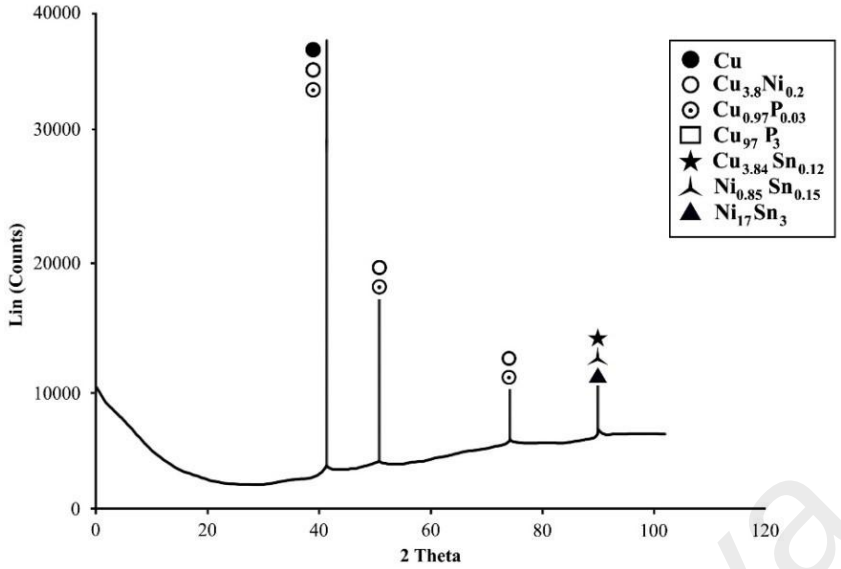

Figure 4.15: XRD pattern of surface brazed at 660 ºC for 15 minutes with marked phase distribution

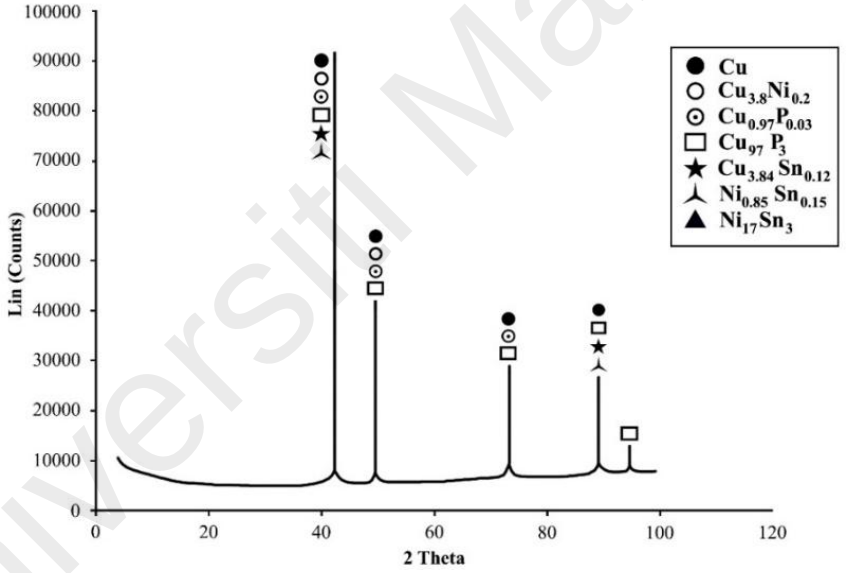

Figure 4.16: XRD pattern of surface brazed at 680 ºC for 15 minutes with marked phase distribution

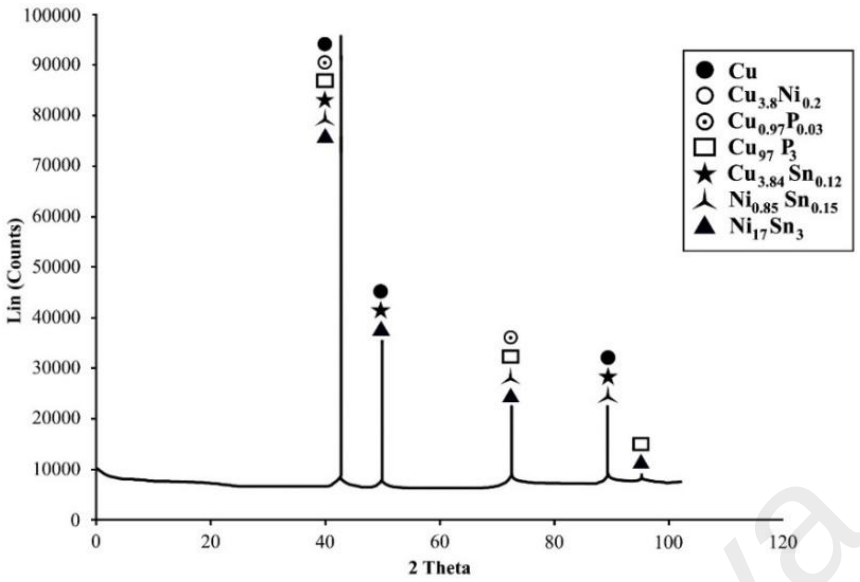

Figure 4.17: XRD pattern of surface brazed at 700 ºC for 15 minutes with marked phase distribution

The XRD analysis indicates that five phases are present due to the reaction of the brazing filler metal with the Cu plate and porous Cu, as follows: Copper Phosphorus ($Cu_{0.97}P_{0.03}$), Copper Phosphide (Cu_{97} P_3), Nickel Tin ($Ni_{17}Sn_3$), Copper Nickel ($Cu_{3.8}Ni_{0.2}$) and Copper Tin ($Cu_{3.84}Sn_{0.12}$). Furthermore, there are strong peaks of $Cu_{0.97}P_{0.03}$ and $Cu_{3.8}Ni_{0.2}$ phases at 660 °C and 680 °C. In sum, the typical joint phase compounds determined include Cu-P, Cu-Ni, Cu-Sn and Ni-Sn. It must also be mentioned that Cu-P alloys are inherently brittle and sensitive to loading rate. Hence, the addition of nominal P content (7 wt.%) slightly affected the reduction of joint ductility. However, phosphorus is often used to deoxidize Cu, which can increase hardness and strength (Sim, 1987).

4.2 Effect of Brazing Parameters on the Mechanical Properties of the Brazed Joints

The mechanical properties of the brazed joints were investigated by performing Vickers microhardness test and compression test.

4.2.1 Microhardness Test

A Vickers microhardness test was performed to evaluate the changes in hardness of the solid and porous Cu after brazing. Indentations were made at several points on the samples from the base to the top side after brazing. The hardness value of the as-received Cu plate prior to brazing was 28.7 HV. The microhardness values of all sample parameters are presented in Figures 4.18 – 4.20.

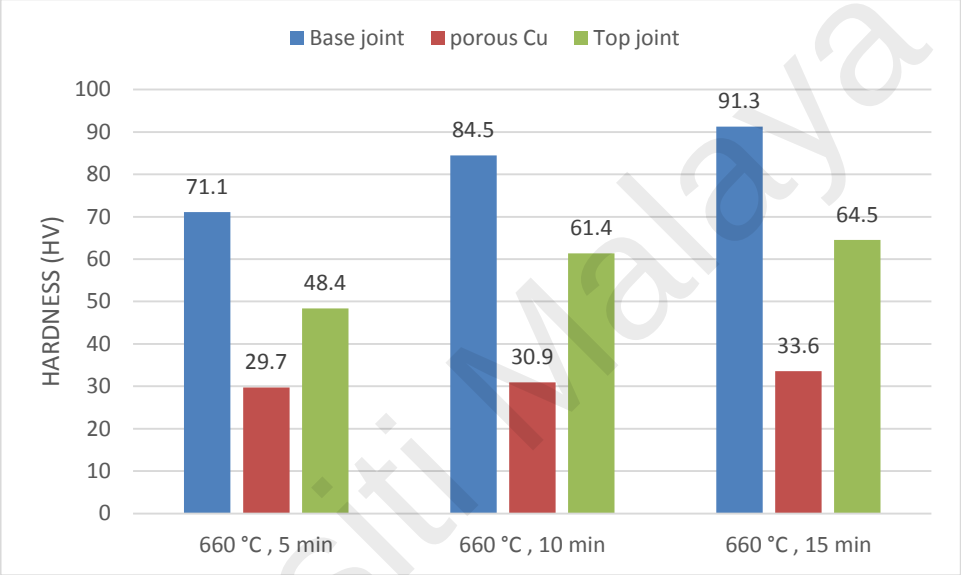

Figure 4.18: Microhardness values of samples brazed at 660 ºC for 5, 10, and 15 minutes holding time

Figure 4.18 shows hardness results for 660 ºC brazing temperature in three categories: base joint, porous Cu and top joint. It is revealed that the base joint hardness value increased to a maximum of 91.3 HV by increasing holding time from 5 to 15 min. The hardness of the porous Cu increased to a maximum of 33.6 HV by increasing holding time to 15 min. The top joint interface shows a gradual increase in hardness to a maximum of 64.5 HV at 15 min holding time. It can be observed that 660 ºC is not suitable temperature parameter due to low hardness values of porous Cu. Furthermore, the hardness of base and top joint increased significantly due to increase in holding time indicating higher holding time is suitable.

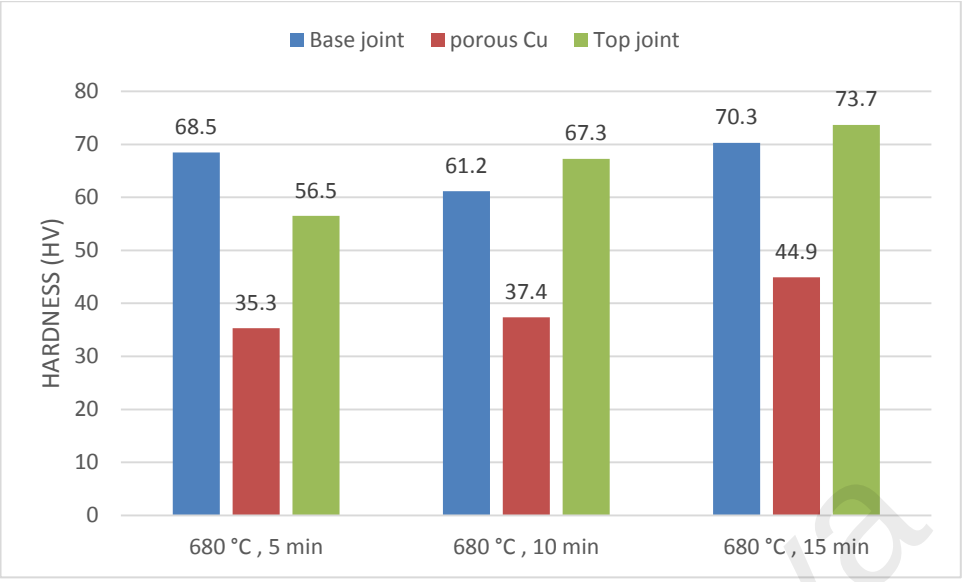

Figure 4.19: Microhardness values of samples brazed at 680 ºC for 5, 10, and 15 minutes holding time

Figure 4.19 indicates that the hardness of porous Cu gradually increased with increasing holding time. The top of the joint had a maximum of 73.7 HV when the holding time was increased to 15 min at 680 °C. The hardness of the base joint brazed at 660 ºC was greater than the base joint brazed at 680ºC, indicating that the filler metal diffused into the porous Cu and top side at 680 ºC. The hardness values of the base of the joint decreased with increasing temperature due to the dissolution and inter-diffusion of the main elements from the filler metal through the porous Cu and the top joint interface. At high brazing temperature, the porous Cu surface hardened significantly and achieved a maximum of 44.9 HV.

Figure 4.20 shows the base joint interface had a maximum value of 99.9 HV at brazing temperature of 700 °C for 5 min holding time. The hardness of the porous Cu increased to a maximum of 46.6 HV as the holding time was increased to 15 min. The top joint interface had a maximum hardness of 68.3 HV when the holding time was increased to 15 min. The hardness values of the base of the joint decreased with increasing holding time due to the dissolution and inter-diffusion of the main elements

from the filler metal through the porous Cu and the top joint interface. This means that the high hardness measured was because of the filler metal residue on the base side.

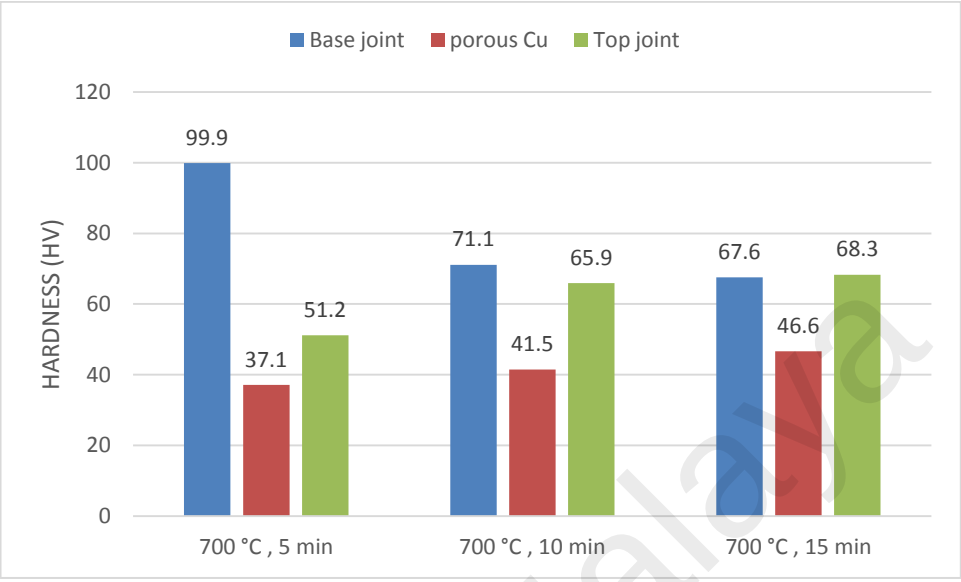

Figure 4.20: Microhardness values of samples brazed at 700 ºC for 5, 10, and 15 minutes holding time

The hardness of porous Cu gradually increased with increasing brazing temperature and time. It is noted that increasing the holding time influenced the hardness values due to interaction between the filler elements and Cu. Overall, as the temperature increased, more diffusion occurred and the hardness values of the porous Cu and top of the joint gradually increased. The diffusion of Ni and P from base side increased as the holding time increased. As a result, the hardness of the base joint decreased due to the dissolution and inter-diffusion of the filler elements into the top joint interface and porous Cu. This is clearly associated with the joint microstructure. The microstructure of the brazed joint consisted of a brittle Cu-P phase, which had an impact on joint ductility (Dahlgren, 1997). However, the Cu-P phase helped increase the hardness values at the joint interface and porous Cu, which in turn increased the rigidity of the porous Cu due to the surface hardening effects. The rigidity of porous Cu after brazing is important to ensure less deformation during servicing of electronics cooling devices.

4.2.2 Compression Test

Compression testing was carried out on three sample parameters to investigate the material behavior under crushing load. The advantage of the compressive stress-strain curve is to elucidate the deformation of materials. For this purpose, compression testing was carried out for samples brazed at 660 ºC, 680 ºC, and 700 ºC for 15 min holding time. The specimens were compressed and the deformation under various loads was recorded. The typical stress-strain curve of all porous samples can be characterized by three distinguished regions known as linear elastic, plateau, and densification (Nakajima, 2007). Figure 4.21 presents the compressive stress-strain curve obtained for porous Cu before brazing. Figure 4.22 – 4.24 presents the results obtained for samples brazed at 660 ºC, 680 ºC, and 700 ºC for 15 min holding time, respectively.

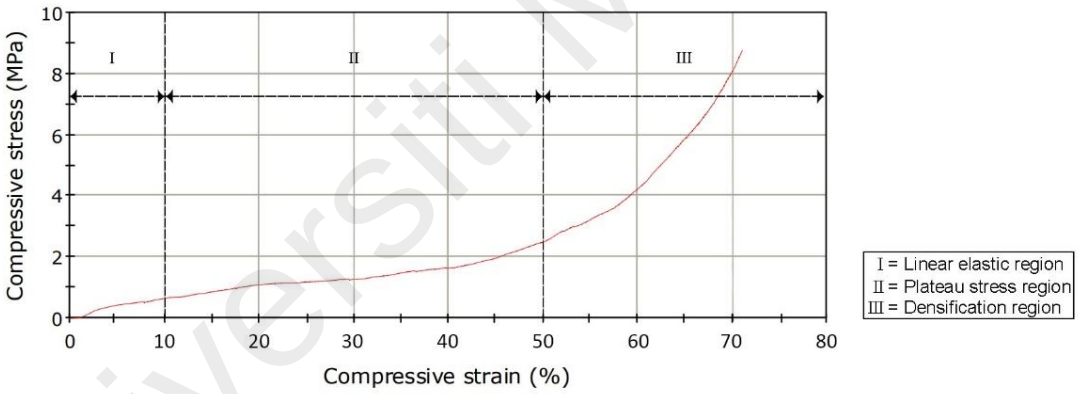

Figure 4.21: Compressive stress-strain curve of porous copper before brazing

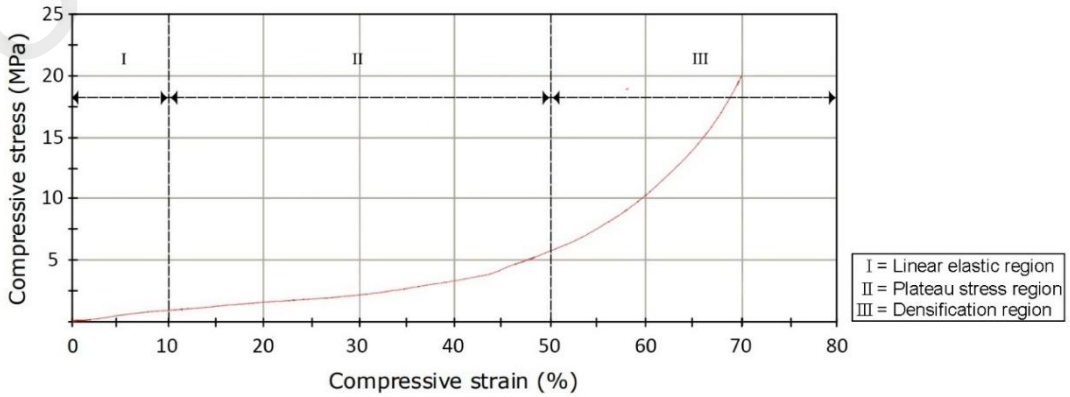

Figure 4.22: Compressive stress-strain curve of sample brazed at 660 ºC, 15 min

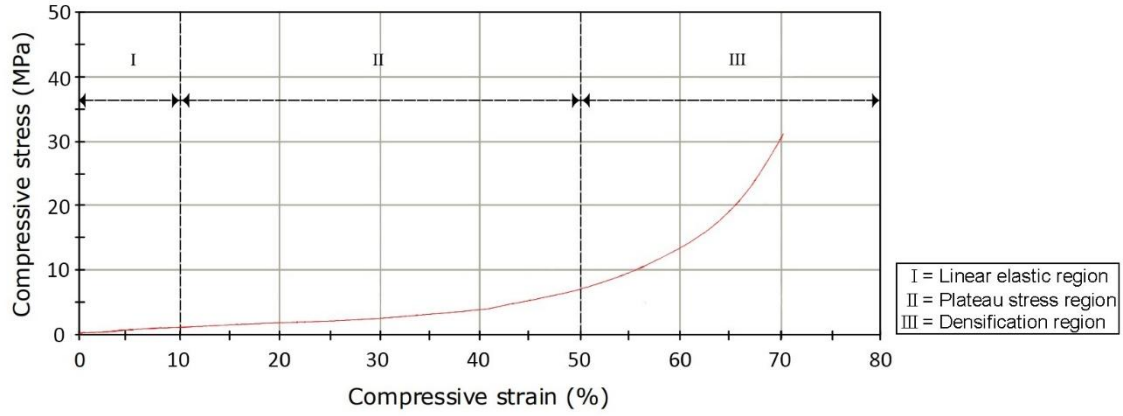

Figure 4.23: Compressive stress-strain curve of sample brazed at 680 ºC, 15 min

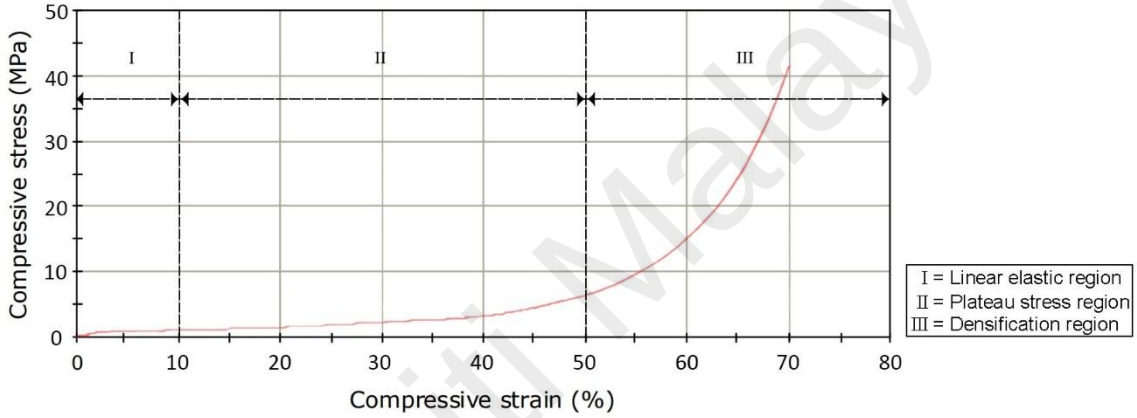

Figure 4.24: Compressive stress-strain curve of sample brazed at 700 ºC, 15 min

In the first region, deformation occurred elastically, presenting a linear development under strains below 10%. The second region shows an almost horizontal development, where stress did not increase remarkably with strain. This region corresponds to the collapse of the cells when the stresses exceeded a certain value and were in a plane perpendicular to the loading direction. The plateau region is a key feature of porous materials, which serves in the case of energy absorption. The energy absorbed by the sample corresponds directly to the area under the stress-strain curve (Gibson & Ashly, 1997). The third region is densification, which manifests under high strains and is where stress increased sharply with increasing strain. As the cell walls come into contact due to increasing deformation, a sharp increase in the stress-strain curve is evident (Ashby, et al., 2000).

Figure 4.21 shows the stress-strain curve of porous copper as received. The porous Cu before brazing had a maximum compressive load of 784 N whereas the compressive stress was 8.4 MPa. As there are limited studies on porous Cu and no studies on compression data, sample porous Cu before brazing is used for comparison with brazed samples. Figure 4.22 shows the sample brazed at 660 ºC for 15 min. The brazed sample had a maximum compressive stress of 20.2 MPa at 70 %. Also, there is a significant increase in plateau stress compared to porous Cu before brazing. As the plateau stress increased for the brazed sample, the energy absorption capacity of the porous Cu increased after brazing.

Figure 4.23 shows the sample brazed at 680 ºC for 15 min. The brazed sample had a maximum compressive load of 2980.9 N, and compressive stress was 31.2 MPa at 70 % compressive strain. Therefore, increasing the temperature increases the maximum compressive stress that porous Cu can withstand. Figure 4.24 shows the sample brazed at 700 ºC for 15 min. The brazed sample had a maximum compressive load of 4240.7 N, and compressive stress was 42.4 MPa at 70 %. The increment in value of compressive stress for the brazed samples confirm that the filler metal diffused into the porous Cu during brazing, hence hardening the porous Cu surface. It also indicates that the porous Cu was able to withstand the highest amount of stress and was more rigid after brazing with increasing brazing temperature. Therefore, it can be concluded that the rigidity of the porous Cu tends to increase because of surface hardening. The rigidity of porous Cu after brazing is essential in ensuring less deformation during cooling device servicing.

CHAPTER 5: CONCLUSION AND RECOMMENDATIONS

This chapter concludes the overall results and discussion made earlier. This chapter also provides recommendations for future studies.

5.1 Conclusion

For all parameters tested, joints were brazed successfully on both sides using a single piece of Cu-P-Ni-Sn brazing filler metal to join porous Cu to Cu substrate. This study of brazing porous copper with copper substrate by using Cu-9.7Sn-5.7Ni-7P (wt.%) shows a significant effect of brazing time and temperature on microstructure and mechanical properties. It was found that this brazing process is economical due to the lower brazing temperature used and shorter holding time. The filler metal was melted, and it filled the joint gap by capillary action to form a joint with good strength. The microstructure of the brazed joint changed with increasing temperature, and no voids or cracks were observed in the sample brazed at 680 ºC for 15 min.

With increasing temperature and time, enhanced diffusion of the filler metal elements was noted in the overall bonded region. The dark grey residual in the filler reaction product reduced at the base and diffused towards the porous Cu and top joint interface. The microstructure of brazing layer changes by the increasing holding time whereby the migration of the P-rich and Ni-rich phases to upper side of the joint was observed. At elevated brazing temperature and time, increased hardness was observed at the porous Cu and the top of the joint due to the presence of abundant filler metal elements identified as reaction products, namely Cu-P, Cu-Ni, Cu-Sn and Ni-Sn. These reaction products are believed to have hardened the porous Cu and brazed joint interfaces, contributing to significant rise in compressive strength and rigidity.

The hardness of the porous Cu increased from 28.7 HV before brazing to a maximum of 46.6 HV at brazing temperature of 700 ºC for 15 min holding time. By increasing the brazing temperature, the maximum compressive strength of the porous Cu increased significantly. The maximum compressive stress obtained at 700 ºC, 15 min was 42.4 MPa whereas the compressive stress before brazing was 8.4 MPa. The increment in value of compressive stress for the brazed samples confirm that the filler metal diffused into the porous Cu during brazing, hence hardening the porous Cu surface. The rigidity of porous Cu is a noteworthy aspect in this study, particularly in terms of its potential application in cooling devices, such as heat exchangers and heat sinks.

5.2 Recommendations

There are several improvements that could be taken to enhance and expand this research in future. The recommendations are described as below:

- The Size of Materials

In this study, the size of the porous Cu and Cu substrate used is slightly smaller. It is suggested to increase the size by 5 mm to further increase the joining area at the base and top side during brazing. A bigger sample size will lead to more joints due to increase in the surface area. This will make it easier to detect and observe the microstructure at the interface.

- Grinding and polishing

Since copper is a soft material, it requires a smooth cutting to avoid any scratches at the surface. Therefore, at the beginning of grinding rough grade sandpaper is used to grind the sample at low speed until a joint at interface is observed. A high-grade sandpaper is preferred afterwards such as 1500, 2000, 2400 and 4000. As for polishing,

it is advised to use alumina micro polish rather than diamond suspension as diamond can damage the sample surface as copper is a soft material

- Brazing parameters (time and temperature)

Based on the experiment, it is found that 660 ºC is not a suitable temperature to join both sides of porous Cu to Cu substrate. Further, none of the parameters was able to completely abolish the dark grey region observed at the joint and porous Cu surface. This can be due to insufficient time or temperature. Therefore, in future investigation it is suggested to increase the temperature or holding time to observe any major differences. It is suggested that the holding time can be further increased to 30 min.

- Shear Strength Test

During the experiment, a compression test was performed to observe the difference in compressive strength of porous Cu. In future study, it is suggested to perform shear test to identify the strength of the joining area between porous Cu/Cu substrate after brazing. This is important for future application purposes.

- Nano-indentation Test

During the experiment, micro hardness test was performed to evaluate the change in hardness of porous Cu. It is suggested to carry out nano-indentation testing to further confirm the results obtained from Vickers micro hardness test.

REFERENCES

American Welding Society (1991) Brazing Handbook (4th Edition) Miami.

Ashby, M.F., Evans, A.G., Fleck, N.A., Gibson, L.J., Hutchinson, J.W., and Wadley, H.N.G. (eds) (2000) *Properties of metal foams* (Chapter 4) Metal Foams, Butterworth-Heinemann, Burlington, pp 40-54

Bangash, M., Ubertalli, G., Saverio, D.D., Ferraris, M., and Jitai, N. (2018) Joining of Aluminium Alloy Sheets to Aluminium Alloy Foam Using Metal Glasses, 8 (8):614.

Bastarows, A.F., Evans, A.G., and Stone, H.A. (1998) Evaluation of cellular metal heat dissipation media (trans: Sciences DoEaA), *Technical Report MECH-325*, Harvard University.

Boomsma, K., Poulikakos, D., and Zwick, F. (2003) Metal foams as compact high-performance heat exchangers, *Mech. Mater. 35*, 1161–1176.

Chiba, H., Ogushi, T., Nakajima, H., and Ikeda, T. (2004) Heat Transfer Capacity of Lotus-type Porous Copper Heat sink, *JSME International Journal*.

Chuan, L., Wang, X.D., Wang, T, H., and Yan, W.M., (2015) Fluid flow and heat transfer in microchannel heat sink based on porous fin design concept, *International Communications in Heat and Mass Transfer*, Vol 65, pp.52-57

Cui, J., Zhai, Q., Xu, J., Wang, Y., and Ye, J. (2014) Adding Sn on the Performance of Amorphous Brazing Fillers Applied to Brazing TA2 and Q235, Journal of Surface Engineered Materials and Advanced Technology 04:342-347.

Dahlgren, A. (1997) Study of International Published Experiences in Joining Copper and Copper alloys. [Online] SKI Report 97:12, Department of Structural Integrity, Swedish Nuclear Power Inspectorate.

Dai, Z., Nawaz, K., Park, Y., Qi, C. and Jacobi, A.M., (2012) A comparison of metal-foam heat exchangers to compact multi-louver designs for air-side heat transfer applications, *Heat Transfer Engineering*, Vol. 33, pp. 21-30

Du, H., Lu, D., Qi, J., Shen, Y., Yin, L., Wang, Y., Zheng, Z., and Xiong, T. (2014) Heat dissipation performance of porous copper with elongated cylindrical pores, *Journal of Material Science and Technology*.

Esmati, K., Omidvar, H., Jelokhani, J., Naderi, M. (2014) Study on the microstructure and mechanical properties of diffusion brazing joint of C17200 Copper Beryllium alloy, *Materials & Design 53*: 766-773

Feng, S., Li, F., Zhang, F., and Lu, T.J. (2017) Natural convection in metal foam heat sinks with open slots, *Experimental Thermal and Fluid Science* 91: 354-362

Fu, W., Song, X.G., Hu, S.P, Chai, J.H., Feng, J.C., and Wang, G.D. (2015) Brazing copper and alumina metallized with Ti-containing Sn0.3Ag0.7Cu metal powder, *Materials & Design 87*: 579-585

Ganjeh, E., Sarkhosh, H., Khorsand, H., Sabet, H., Dehkordi, E.H., and Ghaffari, M. (2012) Evaluate of braze joint strength and microstructure characterize of titanium-CP with Ag-based filler alloy, *Materials & Design 39*: 33-41

Ghosh, R., Kanjilal, A., and Kumar, P. (2017) Effect of type of thermo-mechanical excursion on growth of interfacial intermetallic compounds in Cu/Sn-Ag-Cu solder joints. *Microelectronics Reliability,* 74. (Supplement C):44-51.

Gibson, L.J., and Ashby, M.F. (1997) Cellular Solids: Structure and Properties, Cambridge Solid State Science Series, 2 edn. Cambridge University Press, Cambridge.

Guarino, S., G. Di Ilio, and S. Venettacci, (2017) Influence of Thermal Contact Resistance of Aluminum Foams in Forced Convection: Experimental Analysis, *Materials*, Vol. 10(8): p. 907

Hasap, A., Noraphaiphipaksa, N., and Kanchanomai, C. (2014) The Microstructure and Strength of Copper Alloy Brazing Joints, *Welding Journal* Vol. 93, 116-123.

Hissyam, W.N.W.M.N., Halil. A.M., Kurniawan, T., Ishak, M., and Ariga, T (2017) Effect of Copper-based Fillers Composition on Spreading and Wetting Behaviour, *IOP Conf. Ser.; Mater. Sci. Eng*. **238** 012020.

Hyun, S.K., Nakajima, H., Boyko, L.V., and Shapovalov, V.I. (2004) Bending properties of porous copper fabricated by unidirectional solidification, *Materials Letters 58*, 1082– 1086.

Jacobson, D.M., and Humpston, G. (2005) Principles of Brazing [online], *ASM Internationa*l, Materials Park, Ohio.

Jattakul, P., and Kanlayasiri., K. (2018) In: *MATEC Web of Conferences*: Effects of brazing parameters on the microstructure and tensile shear force of copper sheets using amorphous filler metal.Institue of Technology Ladkrabang, Thailand, 192:01010.

Ji, X., and Xu, J. (2012) Experimental study of the two-phase pressure drop in copper foams, *Int. J. Heat Mass Transfer* 55, 153–164.

Jiang, W., Gong, J.M., and Tu, S.T. (2010) Effect of holding time on vacuum brazing for a stainless-steel plate–fin structure, *Materials & Design 31*(4): 2157-2162.

KalpakjianS, S.S. (2006) Manufacturing Engineering and Technology, 23/25, First Lok Yang Road, Jurong Singapore, Prentice Hall

Kay, D. (2012) Liquation of Brazing filler metals in Brazing, in IBSC 2012: Proceedings from the 5th International Brazing and Soldering Conference, *American Society of Metals*, Las Vegas, Nevada, USA, pp.402-409.

Kiwan, S., Alwan, H., and Abdelal, N. (2020) An experimental investigation of the natural convection heat transfer from a vertical cylinder using porous fins, *Applied Thermal Engineering* 179: 115673

Liu, P.S., and Liang, K.M. (2001) Functional materials of porous metals made by P/M, electroplating and some other techniques, *J. Mater. Sci*. 36, 5059–5072.

Liu, P., Gu, X., Liu, X., Jin, X., Zhang, Y., and Long, Z. (2012) Interfacial reaction of SnAgCu-xNi composite solders on Cu and Ni substrate, In: Gourley R, Walker C (eds) IBSC Proceedings of 5th International Conference, pp 207-212.

Mancin, S., Zilio, C., Diani, A., and Rossetto, L. (2012) Experimental air heat transfer and pressure drop through copper foams, *Exp. Therm. Fluid Sci*. 36, 224– 232.

Miab, J.R., and Hadian, A.M. (2014) Effect of brazing time on microstructure and mechanical properties of cubic boron nitride/steel joints, *Ceramics International 40*(6): 8519-8524.

Miettinen, J. (2001) Thermodynamic description of Cu-Sn-P system in the copper - rich corner. *Calphad* 25. (1): 67-78

Miettinen, J. (2003) Thermodynamic description of the Cu-Ni-Sn system at the Cu-Ni side, *Computer Coupling of Phase Diagrams and Thermochemistry*, Calphad 27 (3):309-318.

Nakajima, H. (2007) Fabrication, properties and application of porous metals with directional pores, *Progress in Materials Science* 52(7): 1091-1173.

Nawaz, K., Bock, J., Dai, Z., and Jacobi, A.M. (2010) Experimental studies to evaluate the use of metal foams in highly compact air-cooling heat exchangers, *Paper presented at the International Refrigeration and Air Conditioning Conference*, Purdue University.

Ogushi, T., Chiba, H., and Nakajima, H. (2006). Development of Lotus-Type Porous Copper Heat Sink, *Materials Transactions*, Vol. 47, No. 9 (2006) pp. 2240 to 2247.

Pradeep, M.K., Balaji, C., and Venkateshan, S.P. (2013) Convection Heat transfer from aluminium and copper foams in vertical channel, *International Journal of Thermal Sciences*.

Predel, B. (1994) Cu-P (Copper-Phosphorus), In: *Madelung O (ed)* Cr-Cs – Cu-Zr. Springer Berlin Heidelberg, Berlin, Heidelberg, pp 1-3

Qu, Z., Wang, T., Tao, W., and Lu, T. (2012) Experimental study of air natural convection on metallic foam-sintered plate, *International Journal of Heat and Fluid Flow 3*8 (Supplement C):126-132.

Rupert, W.D. (1996) Copper-Phosphorus alloys offer advantages in brazing Copper, *Welding Journal*, Vol 75 No.5. pp 43−45.

Schmetterer, C., Vizdal, J., and Ipser, H. (2009) A new investigation of the system Ni–P, *Intermetallics*, 17 (10):826-834

Sekulic, D.P., Dakhoul, Y.M., Zhao, H., and Liu, W. (2008) Aluminum Foam Compact Heat Exchangers: Brazing Technology Development vs. Thermal Performance, In: Proceedings of the Cellmet Conference Dresden.

Shirzadi, A.A., Kocak, M., and Wallach, E.R. (2004) Joining stainless steel metal foams, *Science and Technology of Welding and Joining 9* (3):277-279.

Sim, R.F. (1987) Copper Phosphorus Based (Self-fluxing) Brazing Alloys used for Joining Copper and its Alloys, *FWP Journal*:33 -39.

Soltani, R.T., Mousavi, A.S.A.A., and Atabaki, M.M. (2014) Diffusion brazing of Ti–6Al–4V and austenitic stainless-steel using silver-based interlayer, *Materials and Design* 54: 161–167.

T' Joen, C., Jaeger, D.P., Huisseune, H., Herzeel, V.S., Vorst, N., and Paepe, D.M. (2010) Thermo-hydraulic study of a single row heat exchanger consisting of metal foam covered round tubes, *International Journal of Heat and Mass Transfer 53*, 3262–3274.

Tisha, D., and Indranil, G. (2016) Prospective of employing high porosity open-cell metal foams in passive cryogenic radiators for space applications, *IOP Conf. Ser.: Mater. Sci. Eng,* Vol. 171 012048.

Tuchinskiy, L. (2005) Novel fabrication technology for metal foam, *J. Adv. Mater*. 37, 60–65.

Vesenjak, M., Kovačič, A., Tane, M., Borovinšek, M., Nakajima, H., and Ren, Z. (2012) Compressive properties of lotus-type porous iron, *Computational Materials Science 65*(0): 37-43.

Wang, J., Kong, H., Xu, Y., and Wu, J (2019) Experimental investigation of heat transfer and flow characteristics in finned copper foam heat sinks subjected to jet impingement cooling, *Applied Energy*, Vol. 241, pp. 433-443.

Xiao. Z., and Zhao, Y. (2013). -Tubío, R. I., Pérez, J., Ferreiro, S., and Aldegunde, M. (2007). Heat transfer coefficient of porous copper with homogeneous and hybrid structures in active cooling, *J. Mater. Res.*, Vol. 28, No. 17, Sep 14.

Zaharinie, T., Moshwan, R., Yusof, F., Hamdi, M., and Ariga, T. (2014) Vacuum brazing of sapphire with Inconel 600 using Cu/Ni porous composite interlayer for gas pressure sensor application, *Materials & Design 54*(0): 375-381

Zahri, N.A.M., Yusof, F., Ariga, T., Haseeb, A.S.M.A., Mansoor, M.A., and Sukiman, N.L (2019) Open-cell copper foam joining: joint strength and interfacial behaviour, *Mater. Sci. and Tech,* 35:16. 2004-2012

Zhang, L., Mullen, D., Lynn, K., and Zhao, Y. (2009). *Materials Research Society, 1188:* 1188-LL04-07.

Zhang, H., Chen, L., Liu. Y., and Li, Y. (2013). Experimental study on heat transfer performance of lotus-type porous copper heat sink, *International Journal of Heat and Mass Transfer 56*: 172–180.

Zhang, J., Wang, T., Liu, T., and He, Y. (2014) Effect of brazing temperature on microstructure and mechanical properties of graphite/copper joints, *Materials Science & Engineering*, 26-3.

Zhang, J., Yu, W., and Lu., W. (2016) Mechanical Properties and Microstructure of Pure Copper Joints Brazed with Amorphous Cu68.5Ni15.7Sn9.3P6.5 Filler Metal. *International Journal of Simulation Systems Science & Technology* 17, No. 24.

Zhang, Y., Long, E., and Zhang, M. (2018) Experimental study on heat sink with porous copper as conductive material for CPU cooling, *Materials Today; Proceedings* 5: 7 15004-15009

Zhao, C.Y., Lu, W., and Tassou, S.A. (2009) Flow boiling heat transfer in horizontal metal foam tubes, J. Heat Transfer 131, 99 121002-1–8

Zhaoda, Z., Meng, L., Li, X., Zhang, G., Xu, Y., and Deng, J. (2020) Enhanced heat transfer performance of optimized micro-channel heat sink via forced convection in cooling metal foam attached on copper plate, *J. of Energy Storage* 30:101501

Zorc, B., and Kosec, L. (2000) Comparison of brazed joints made with BNi-1 and BNi-7 nickel-base brazing alloys. *Revista de Metalurgia* 36:100-107.

LIST OF PUBLICATIONS AND PAPERS PRESENTED

Article Published

Sami, M.M.; Zaharinie, T.; Yusof, F.; Ariga, T. Investigation on Strength and Microstructural Evolution of Porous Cu/Cu Brazed Joints Using Cu-Ni-Sn-P Filler. *Metals* **2020**, *10*, 416. https://doi.org/10.3390/met10030416 (Indexed in WOS/Science Citation Index)

Article Accepted

Sami, M.M., Zaharinie, T., Yusof, F., and Ariga, T. (2020) Effects of Brazing Parameters on the Microstructural and Mechanical Properties of a Porous Copper Heatsink, Special issue on Green Manufacturing Processes and Systems. (Scopus Index)

Conference Proceedings

Sami, M.M., Zaharinie, T., Yusof, F., and Ariga, T. (2018) Investigation on Microstructural and Mechanical Properties of Porous Copper Heat Sink, Proceedings of Mechanical Engineering Research Day 2018, pp. 248-250 (Indexed in WOS/CPCI).

Zaharinie, T., Sami, M.M., Yusof, F., and Ariga, T. (2016) Temperature effects on microstructures of brazing porous copper to copper using Cu-based filler metal, LÖT.

Sami, M.M., Zaharinie, T., Yusof, F., and Ariga, T. (2016) Effects of Brazing Parameters to Microstructure and Mechanical Properties of Brazing Porous Copper to Copper, In Advances Processes and Systems in Manufacturing: An International Conference 2016, pp. 43-44 (Indexed in WOS/CPCI).